NAA-SR-5991
COPY

PRELIMINARY RESULTS OF THE SNAP 2 EXPERIMENTAL REACTOR

AEC Research and Development Report

ATOMICS INTERNATIONAL
A DIVISION OF NORTH AMERICAN AVIATION, INC.

DISCLAIMER

NAA-SR-5991
SPECIAL
60 PAGES

PRELIMINARY RESULTS OF THE SNAP 2 EXPERIMENTAL REACTOR

By
STAFF OF
COMPACT POWER SYSTEMS DEPARTMENT

Edited by
M. W. HULIN
J. BEALL

ATOMICS INTERNATIONAL
A DIVISION OF NORTH AMERICAN AVIATION, INC.
P.O. BOX 309 CANOGA PARK, CALIFORNIA

CONTRACT: AT(11-1)-GEN-8
ISSUED: APRIL 1, 1961

BLANK

CONTENTS

		Page
	Abstract	vii
I.	Introduction	1
II.	SER Physical Description	3
	A. Reactor Core	3
	B. Reactor Core Vessel	7
	C. Reactor Containment Vessel	8
	D. Reactor Shielding	9
	E. Primary NaK Coolant System	9
	F. Secondary NaK Coolant System	13
	G. Auxiliary Systems	13
III.	Instrumentation and Control System	18
	A. Nuclear Instrumentation	18
	B. Process Instrumentation	18
	C. Control Console	18
IV.	SER Operation	21
	A. Highlights of SER Operation	21
	B. Maintenance Problems	24
V.	SER Tests	28
	A. Reactivity Override Tests	28
	B. Stability and Safety Tests	28
	C. The Cold, Clean, Excess Reactivity	28
	D. Worth of the Control Elements	30
	E. The Temperature Defect	34
	F. The Power Defect	34
	G. Equilibrium Xenon Defect	35
	H. Long-Term Loss Rate	35
	I. Summary of Parameters Pertinent to the Override of Reactivity Losses	37
	J. Safety Element Worths	37
	K. Safety Element Drop Times	38
	L. Temperature Coefficients	38
	M. Comparison of Calculated and Measured SER Parameters	46

CONTENTS

		Page
VI.	Proposed Tests	47
	A. Static Power Coefficients	47
	B. Grid Plate Coefficients	48
	C. Reactivity Oscillations	49
	D. Reflector Coefficient Test	51
	E. Hydrogen Losses	52
	F. Control Drum Calibration	52
VII.	Conclusions	53
	References	54

TABLES

I.	SER Chronology	2
II.	Calculated Excess Reactivity Requirements	7
III.	SER Parameters	15
IV.	Summary of SER Operation	22
V.	Scrams	24
VI.	Total Control Element Worths, Dry Core	31
VII.	Control Element Worths, Wet Core (5932 kwh Energy Release)	31
VIII.	Control Element Worths, Wet Core (147,358 kwh Energy Release)	33
IX.	Loss Rates	36

FIGURES

1.	Fuel-Moderator Element Assembly	4
2.	Fuel Element Lattice	4
3.	Radial Reflector Cross Section	5
4.	Control Drum and Safety Element Drive Mechanism	6
5.	Reactor Installation	8
6.	SER Building, Plan View	10
7.	SER Building, Elevation View	11

FIGURES

		Page
8.	NaK Coolant Flow Diagram	12
9.	Nuclear Instrumentation	19
10.	Range of Operation of Neutron Detectors	20
11.	SER Operation at Various Core Coolant Temperatures	22
12.	SER History	23
13.	Excess Reactivities for Various Fuel Loadings	29
14.	Control Drum No. 1, Comparison of Drum Worths After 141,100 kwh of Operation	32
15.	Control Drum No. 2, Comparison of Drum Worths After 141,100 kwh of Operation	32
16.	Control Drum No. 3, Comparison of Drum Worths After 141,100 kwh of Operation	33
17.	SER Data, Temperature Defect From Data of Experiments on December 19, 1959	34
18.	SER Xenon Transient Experiment	35
19.	Measured Loss Rate vs Average Core Temperature	36
20.	Typical Safety Element Worth Curve	38
21.	Temperature Coefficient ($\Delta\rho/\Delta T$) vs Average Core Coolant Temperature	41
22.	SER Power Coefficient	42
23.	SER Power Coefficient vs Average Core Temperature	42
24.	Ramp Insertion Experiment, kw vs Time	43
25.	Ramp Insertion Experiment, Reactor Temperature vs Time	44
26.	Reduction of Static Power Coefficient Measurements	49
27.	Estimated Response to Coolant Temperature Change	52

PRINCIPAL COMPARISONS		
Parameter	Calculated	Measured
Critical Mass (kg)	2.9	3.0
Excess Reactivity ($)	7.77	9.78
Temperature Defect ($) (at 200 to 1100°F core average temp.)	-3.10	-3.42
Prompt Temperature Coefficient (¢/F°)	-0.2	-0.05
Overall Temperature Coefficient (¢/F°)	-0.27	-0.35
Xenon Defect ($) (equilibrium at 50 kw)	-0.36	-0.39
Reactivity Loss Rates (¢/day) (at 50 kw, & 1100°F core average temp.)	-0.41	-0.79
Fuel Element Worth in Outer Ring ($)	1.31	1.40
Maximum Fuel Temperature (°F) (at 50 kw)	1250	1270
Control Drum Worth ($) (at 0 to 180° rotation, with one drum)	2.50	3.92

ABSTRACT

This report presents the operating history of the SNAP 2 Experimental Reactor (SER) and the preliminary results from the testing program. The total energy generated during the life of the reactor was 224,650 kilowatt hours. This is equivalent to approximately one-half year of full-power operation. The methods used to obtain the reactor parameters are also described. The experimental data obtained were generally in excellent agreement with calculated values. The principal comparisons are tabulated. (See page vi.)

I. INTRODUCTION

Compact, lightweight power systems are being developed to supply auxiliary power to orbiting space vehicles over an extended period of time. The SNAP-2 Experimental Reactor (SER) is the first of a series of nuclear reactors in this program. Its primary purpose is to test the reactor core under design power and temperature conditions.

This reactor concept combines the advantages of the homogeneous thermal reactor with those of a heterogeneous reactor: i. e., the clad fuel-moderator rods prevent fission products from contaminating the coolant and the homogeneous fuel-moderator tends to increase the thermal utilization factor, f, increasing the value of k, the neutron multiplication factor. The fuel-moderator is a hydride uranium-zirconium alloy enriched in U^{235}, which is formed into rods and canned in thin-walled, stainless steel tubes. Before final assembly, the inside surfaces of the tubing are coated with a vitreous enamel to reduce hydrogen diffusion. Heat is removed from the core by a eutectic NaK (78 wt % potassium) coolant which flows upward between the fuel elements. The resultant core is compact, lightweight, and capable of producing the high-temperature conditions required to operate power conversion units in space. The feasibility of this concept was indicated by results of experiments with the SNAP-2 Critical Assembly. The SER has proven the practicality of the design under full-power operating conditions of 50 kw and at the designed coolant outlet temperature of 1200°F. This reactor is located in the Burro Flats area of the Santa Susana Field Test Site of Atomics International approximately 30 miles northwest of Los Angeles.

Many of the components and systems used in the SER contain unique features or were operated under unusual environmental conditions; therefore, a comprehensive testing program was developed to precede actual operation. This testing program included:

a) A critical assembly to check the methods of calculation used for nuclear design and to obtain, experimentally, the control and safety element worths, excess reactivity, neutron lifetime, and other nuclear and physical parameters of the SER configuration.

b) The coolant loop mockup was used to check the SER heat removal system.

c) Performance tests of the safety and control elements with their related instrumentation were tested under expected operating conditions.

d) A program to investigate the radiation stability of the fuel-moderator material.

e) A program to investigate the physical properties of the fuel-moderator and cladding materials.

Efforts in the areas covered by Items d and e continue in parallel with the SER operation. Table I presents a chronological record of the SER.

TABLE I

SER CHRONOLOGY

Item	Date
Construction started	June 1958
Facility completed	March 1959
Dry critical	September 19, 1959
Wet critical	October 20, 1959
First power operation	November 5, 1959
First operation at design power and temperature	November 9, 1959
Reactor completed 1000 hr continuously at design temperature and power	April 23, 1960
Final shutdown	November 19, 1960

Section II of this report provides a brief description of the design features and performance characteristics of the SER reactor system. Section III is a discussion of the instrumentation and control systems. The operation history of the SER is covered in Section IV. A detailed description of reactor tests and a discussion of their results are covered in Section V. The proposed test program subsequent to August 1960 is covered in Section VI. Section VII contains the conclusions and appraisal of the SER from operating experience to November 19, 1960.

II. SER PHYSICAL DESCRIPTION

The reactor system and its enclosure are described in References 1 and 2. The heat transfer system is comprised of two NaK loops with an intermediate heat exchanger. Heat removed from the core by NaK in the primary loop, which becomes radioactive, is transferred to the secondary loop through the intermediate heat exchanger. Heat from the secondary loop which is not radioactive is dissipated to the atmosphere through the airblast heat exchanger. The reactor is installed within a containment vessel below ground level, in which an inert nitrogen atmosphere is maintained. Biological shielding in the top of the containment vessel protects personnel during the time the reactor is in operation. The radioactive primary sodium system and the intermediate heat exchanger reside in a shielded vault with a nitrogen atmosphere. The secondary NaK system and airblast heat exchanger are exposed to air atmosphere.

A. REACTOR CORE

The reactor core is comprised of 61 fuel-moderator rods – 93.12 wt % $ZrH_{1.70}$ and 6.88 wt % of 93% enriched U alloy. This material contains a minimum of 6×10^{22} atoms of H/cc (compared to cold water with 6.7×10^{22} H atoms/cc). Each fuel-moderator element consists of a solid rod 0.975 in. in diameter by 10 in. long with a 0.975-in. diameter by 1-1/2 in. long Be slug at each end, and is canned in a 1-in. OD, 10-mil wall thickness, stainless steel tube. The tube is sealed at each end by welding in, 1/2 in. stainless steel end caps. The inside surface of the stainless steel tubing is coated with a 2 to 3 mil layer of boron-free vitreous enamel. The fuel-moderator element has a total length of 14 in. and is shown in Figure 1.

The 61 elements are arranged on 1.015 in. centers in a triangular lattice to form a hexagonal core approximately 8 in. across the flats and 9 in. across the corner as shown in Figure 2. The void between the hexagonal fuel lattice and 9-in. ID core vessel was filled with 6 Be shims; and the core vessel is surrounded by Be reflector sections approximately 3 in. thick as shown in Figure 3. The reflector is composed of 6 sections – 3 semicylindrical control drums and 3 fall-away type safety elements.

End reflection is achieved with the Be end plugs and the stainless steel weld plugs together with the NaK coolant plenums and the grid plates. The reactor is

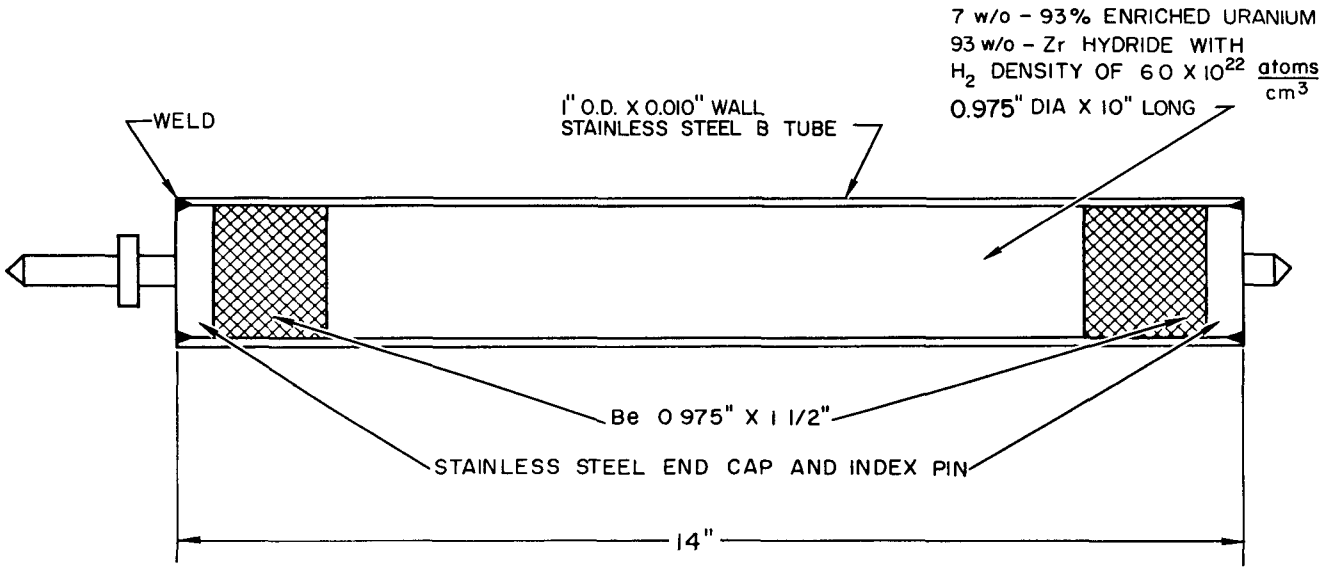

Figure 1. Fuel-Moderator Element Assembly

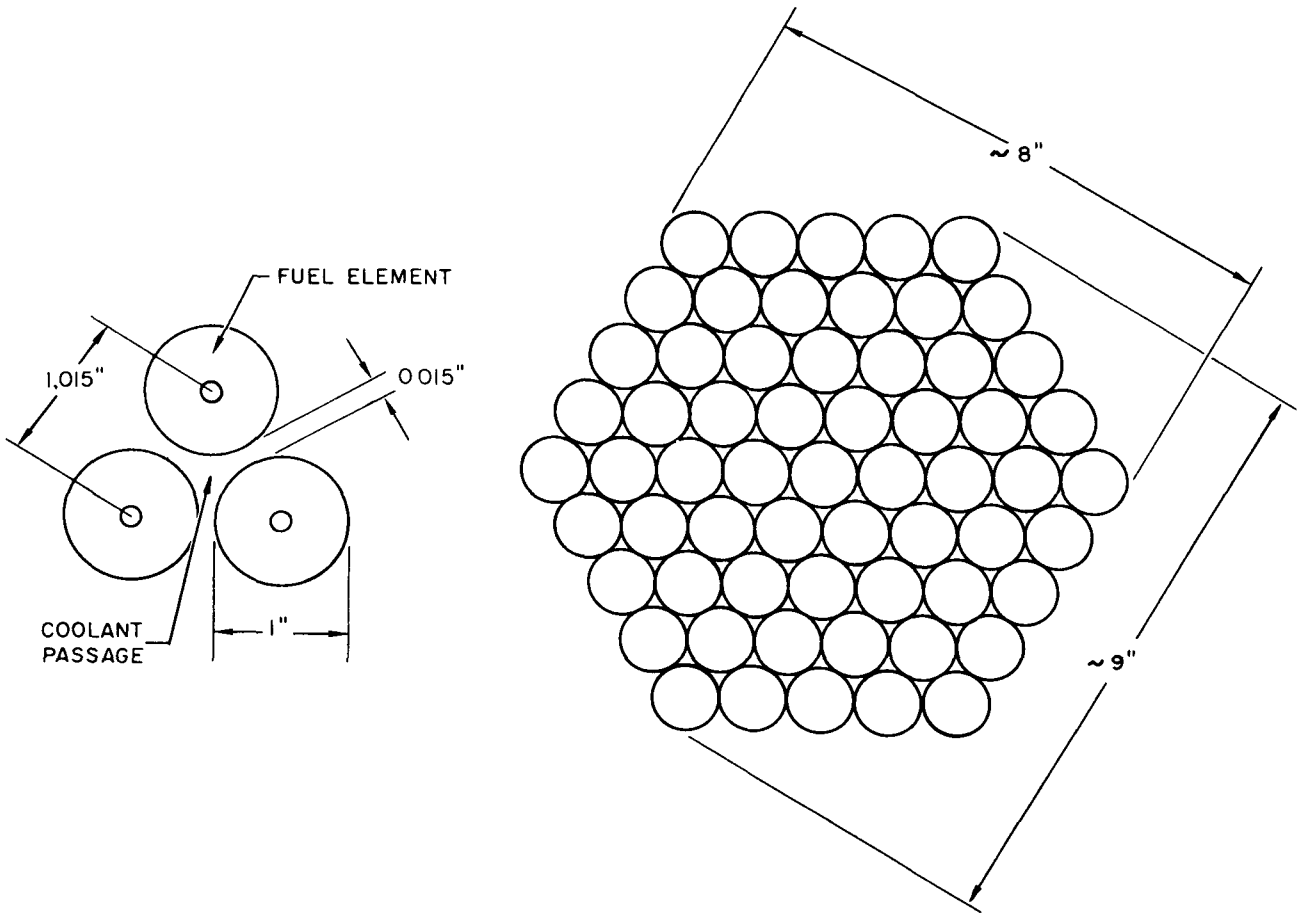

Figure 2. Fuel Element Lattice

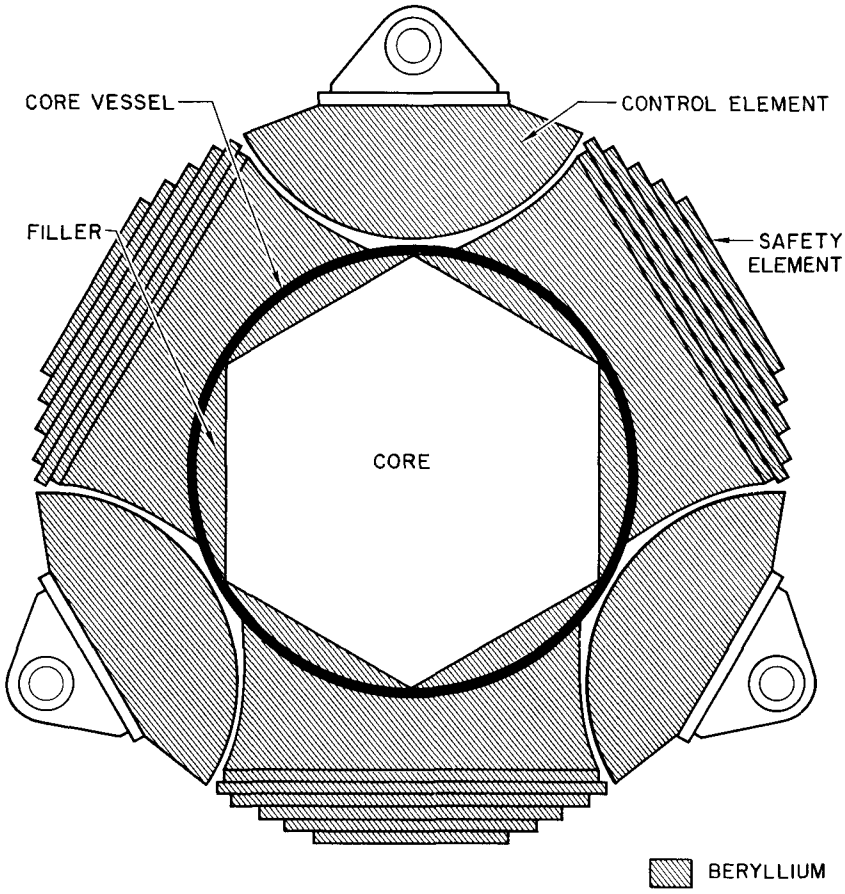

Figure 3. Radial Reflector Cross-Section

controlled by rotating external portions of the radial reflector away from the core, thus changing the effectiveness of the reflector for maintaining neutron economy.

Each control drum is driven with a direct motor drive geared to provide a maximum insertion rate of 2.5¢/sec. Each control drum has a total worth of about $3.65 over the range 0 to 180°. A Selsyn readout system provides visual observation of the position of each control drum. The control drum drive mechanisms and position indicators are located behind shielding to protect them from the high neutron and gamma radiation; the control drums do not scram.

Each safety element is pivoted at the bottom, and safety shutdown of the reactor is achieved by allowing the safety elements to fall by gravity away from the core. Each of the three independent safety elements is worth about $5.40 in reactivity. The safety element drive mechanism and the control drum drive mechanism are shown in Figure 4. Each safety element is moved into position

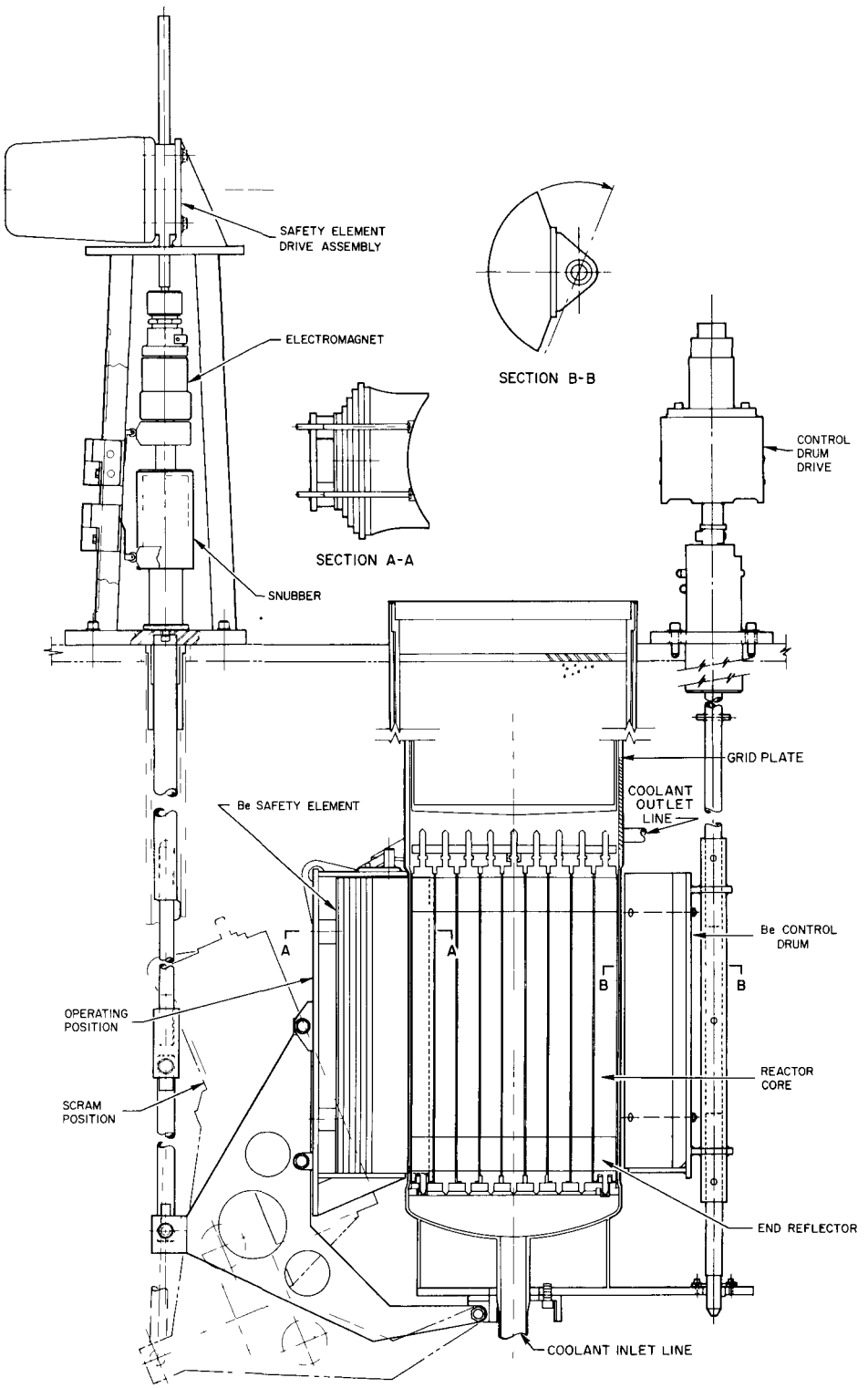

Figure 4. Control Drum and Safety Element Drive Mechanism

by means of a rack-and-pinion system attached by a magnet to the pull-up rod. The safety elements are scrammed by interrupting power to the magnets. The reactivity insertion rate is limited to about 6¢/sec.

A Pu-Be neutron source is mounted on a bracket at the base of one of the control drums.

During the critical experiments, the excess reactivity of the cold reactor was adjusted to 4% ($4.77) by mechanically limiting the inward rotation of the control drums. The results of calculations of the excess reactivity requirements are summarized in Table II.

TABLE II

CALCULATED EXCESS REACTIVITY REQUIREMENTS

	%	$
Xenon and samarium buildup	0.3	0.36
Temperature override (200 to 1100°F)	2.0	3.10
Fuel depletion and fission products	0.05	0.06
Hydrogen loss	1.5*	1.79
Operating excess	0.15*	0.18
	4.0	5.49

*Estimated.

B. REACTOR CORE VESSEL[1]

The core vessel is a cylinder 9-1/2 in. in diameter with a wall thickness of 3/32 in. The overall length is 16-3/8 in. The core vessel is penetrated at the bottom and the top by 1-1/4-in. coolant lines, on the bottom by the inlet line, and on the side by the outlet line above the top grid plate.

The core vessel contains the upper and lower grid plates for positioning and holding the fuel-moderator assemblies and a top hat above the upper grid plate to control flow through the core. The grid plates also allow for flow of NaK coolant through the fuel rod interstices and around the reactor core. Figure 4 shows the grid plates in relation to the reactor core vessel.

C. REACTOR CONTAINMENT VESSEL[1]

A 3/4-in. boiler plate carbon steel containment vessel, Figure 5, containing the reactor components and the necessary shielding is located below ground level. The vessel is 15 ft, 5-5/8 in. deep and reduces in three steps from 48 in. ID at the top to 38-in. ID at the bottom. Water circulated through cooling coils around the outside of the containment vessel removes the excess heat and prevents overheating of the surrounding concrete. Nitrogen, at slightly above atmospheric pressure, is used as a cover gas to exclude air from the vessel and

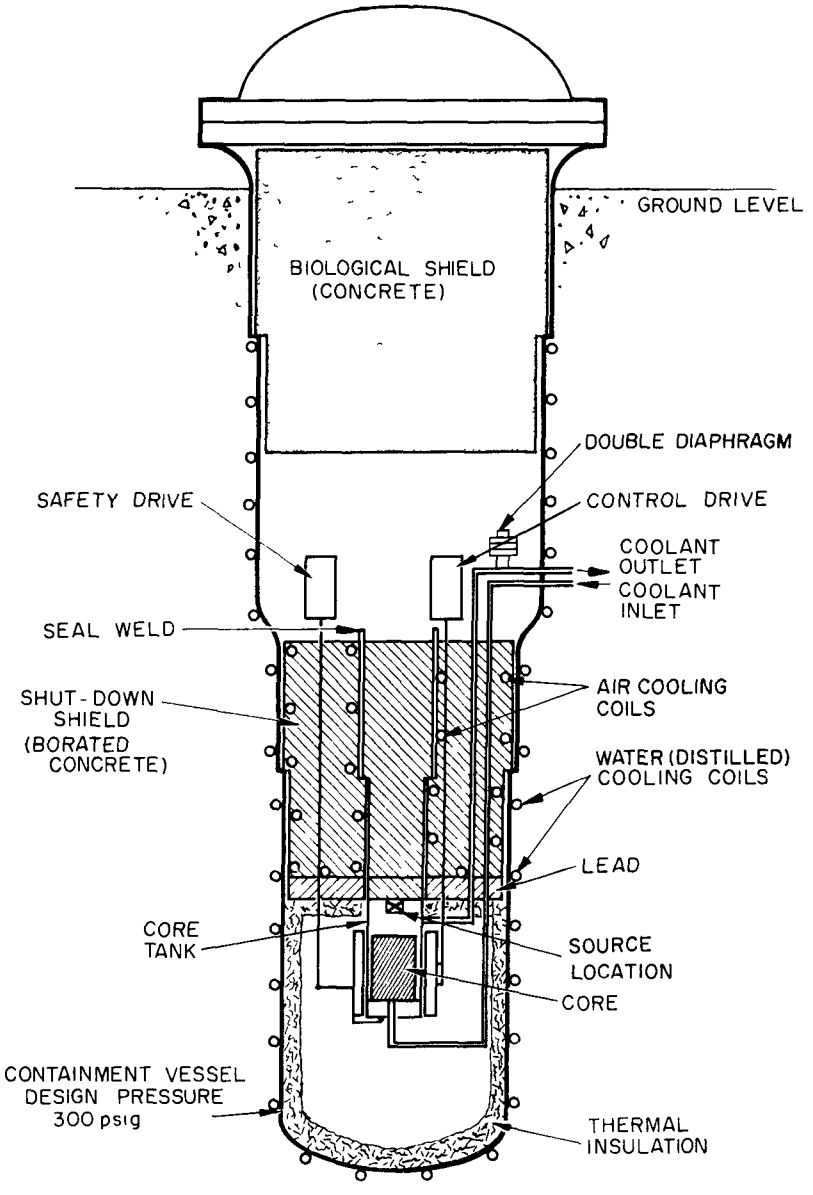

Figure 5. Reactor Installation

thus minimize the possibility of sodium fires and hydrogen-oxygen reaction. In the event of a rupture of the core tank, the fission products would be retained by the containment vessel.

The containment vessel was designed for a pressure of 305 psig and was hydrostatically tested at 456 psig in accordance with the ASME Boiler and Pressure Vessel Code for unfired pressure vessels containing lethal substances.

A calibrated rupture diaphragm, set to rupture at 150 psi, is connected to the primary coolant system and is located within the containment vessel, Figure 5. The diaphragm is installed to ensure that no rupture of the system would occur outside this vessel.

D. REACTOR SHIELDING[1]

The reactor shielding consists of three parts: (1) the shutdown shield above the core, (2) the biological shield which seals off the containment vessel, and (3) the concrete and earth around the containment vessel.

The shielding has been designed for the resultant radiation dose levels from operation at 100 kw (twice the designed power level) as follows:

Accessible Area Above the Heat Exchanger	3.6 mr/hr
Accessible Area Above the Core	0.8 mr/hr

E. PRIMARY NaK COOLANT SYSTEM[1]

The bulk of the primary NaK coolant system is located within a shielded, sealed-off vault. The internal dimensions of the vault are 9-1/2 ft long, 8 ft wide, and 7 ft high. The location of the primary loop vault with respect to the reactor core, the equipment pit, and the secondary NaK coolant system is shown in Figures 6 and 7. A simplified flow diagram of the primary, secondary, and auxiliary NaK systems is shown in Figure 8.

The principal components of the primary NaK coolant system are the fill-and-drain tank, the primary surge tank, the intermediate counter-flow heat exchanger, the electromagnetic pump, the primary flowmeter, the electrical heater, the plugging indicator, the valves and valve operators, and the piping and thermal insulation.

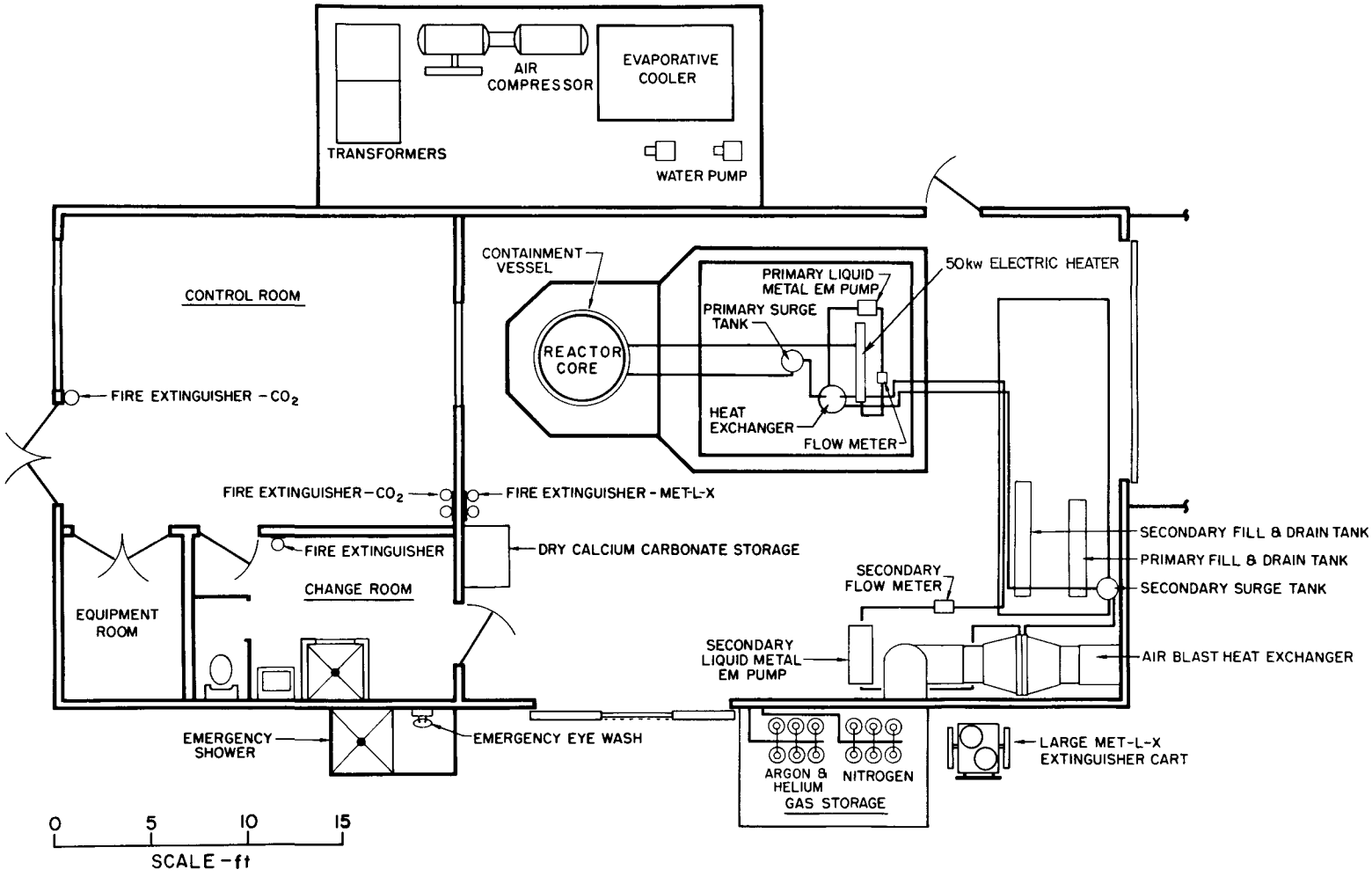

Figure 6. SER Building, Plan View

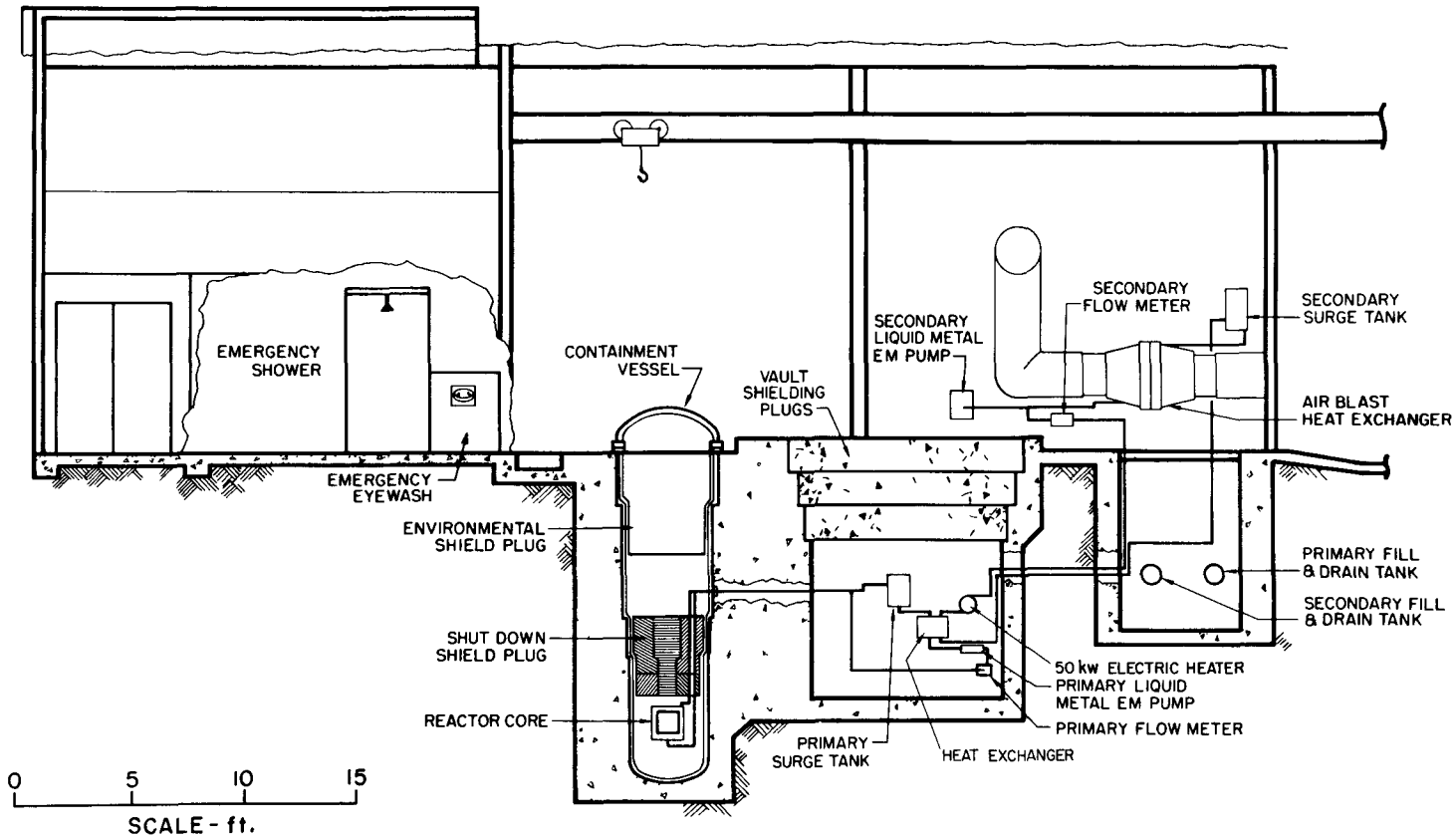

Figure 7. SER Building, Elevation View

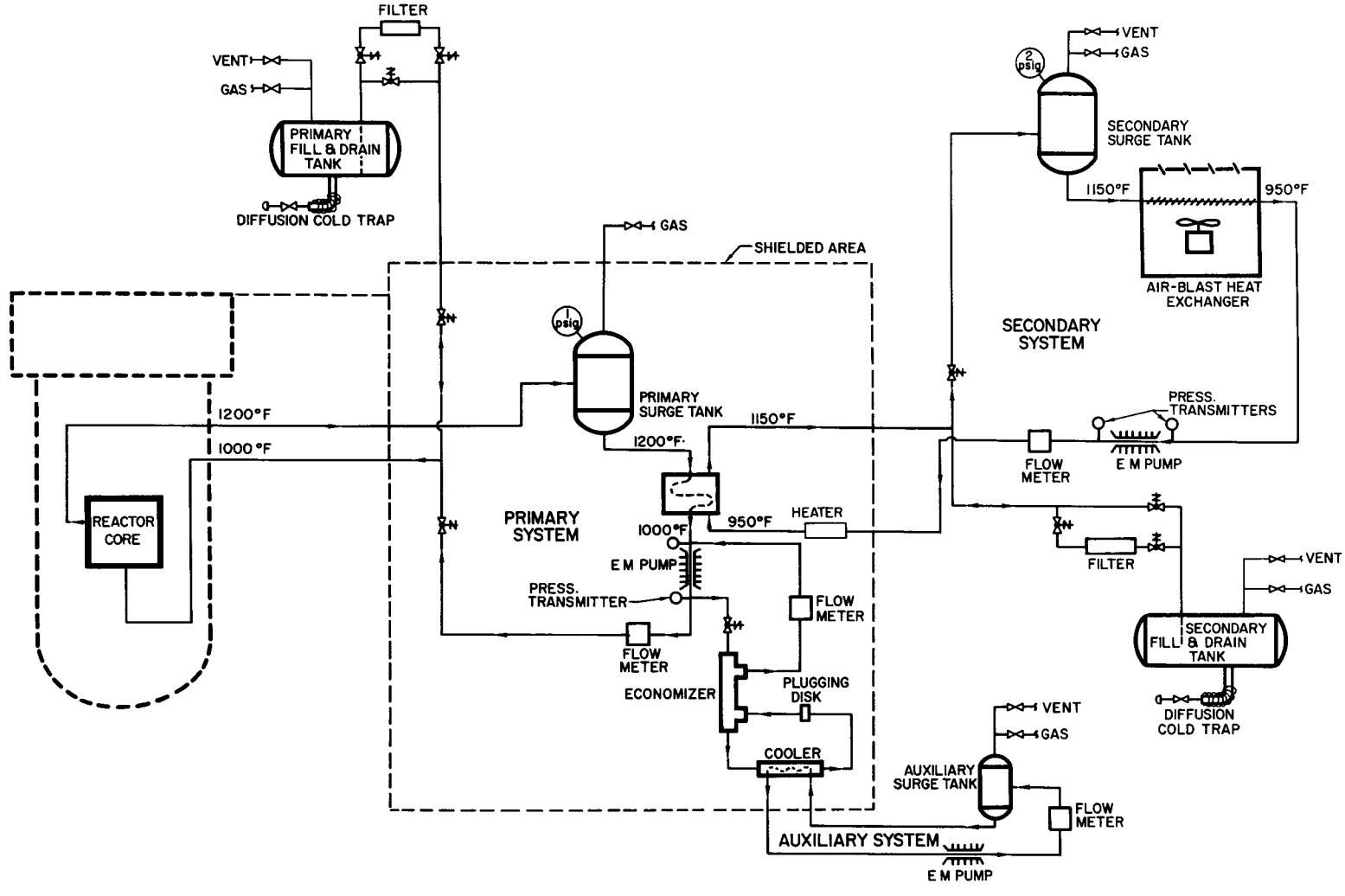

Figure 8. NaK Coolant Flow Diagram

F. SECONDARY NaK COOLANT SYSTEM[1]

The function of the secondary NaK coolant system is to transfer the heat from the primary radioactive NaK to the secondary nonradioactive NaK and then to dump this heat to the atmosphere by means of an airblast heat exchanger. The heat exchange from primary to secondary NaK is accomplished in the intermediate heat exchanger located within the shielded vault. The secondary inlet and outlet NaK lines of the intermediate heat exchanger pass through sleeves in the vault wall bordering the equipment pit. These lines lead into and out of the pit to join that portion of the secondary coolant system located at the ground floor level.

The principal components of the secondary NaK coolant system are the secondary fill-and-drain tank, the secondary surge tank, and airblast heat exchanger, the electromagnetic pump, the secondary flowmeter, valves, piping, and insulation.

G. AUXILIARY SYSTEMS

1. Auxiliary NaK Coolant System

An auxiliary NaK coolant system, Figure 8, is utilized to provide a coolant for the plugging indicator used to monitor the oxygen and/or hydrogen content of the primary NaK coolant. The pump, surge tank, and flowmeter for this auxiliary loop are located in the equipment pit. NaK lines which pass through sleeves located in the primary vault wall are for circulating auxiliary NaK through the shell side of the plugging indicator cooler. A fill-and-drain tank is not required for this system.

2. Helium Gas System

Helium is now used as a cover gas in the surge tank and in the fill-and-drain tank of the primary system. Argon was originally used in the primary system; however, because argon becomes radioactive in passing through the reactor (either from entrained gas bubbles or because argon becomes slightly soluble in high temperature NaK), it was replaced with helium.

Transfer of NaK from the primary fill-and-drain tank is accomplished by pressurizing with helium. Draining the NaK is similarly accomplished by pressurizing the surge tank with helium. All helium vented from the primary system is collected in a storage tank designed for 300 psi operation. The gas

is monitored for activity prior to release through the common vent which exhausts several feet above the reactor building.

3. Argon Gas System

Argon is used as a cover gas in the surge tanks of the secondary and auxiliary NaK systems as well as in the secondary fill-and-drain tank. In addition, it was used to purge the liquid metal systems prior to filling these with NaK. Transfer of NaK from the secondary fill-and-drain tank to the secondary system is accomplished by pressurizing with argon. Draining the NaK from the systems is similarly accomplished by pressurizing the surge tank with argon.

4. Nitrogen Gas System

Nitrogen gas is used for maintaining an inert atmosphere within the containment vessel and within the primary loop vault. A positive nitrogen pressure of 1/2 in. water is maintained in the containment vessel and the primary vault during reactor operation. Venting of the nitrogen system is via the vent used for the argon supply. Venting is required to control the moisture and oxygen content in either the containment vessel or the primary vault and to regulate the pressure as the system undergoes temperature change.

5. Water Cooling System

The function of the water cooling system is to maintain low temperatures in the concrete surrounding the reactor containment vessel and in the concrete walls of the primary loop vault. A closed-cycle distilled water system with hydrogen addition is used to control the buildup of scale deposits within the cooling coils. Cooling of the circulating distilled water is by a spray-type, forced-draft, evaporative cooler located on the equipment pad outside of the reactor building.

6. Air Cooling System

Cooling of the shutdown shield assembly within the reactor containment vessel is accomplished by air flow from the air cooling system. A positive displacement rotary-type air compressor driven by a 25-hp motor is located on the equipment pad outside the reactor building. A drier installed at the compressor discharge ensures the delivery of dry air to the various cooling coils. Exhaust from the cooling system is vented several feet above roof height along with the argon, helium, and nitrogen. All vent gas is monitored periodically to ensure

that activity released to the surrounding terrain is less than the maximum permissible concentration.

TABLE III

SER PARAMETERS[1,2,3]

Core Composition	
Fuel loading	3.0 kg U^{235}
Number of fuel-moderator elements	61
Composition of fuel-moderator elements	6.88 wt % of 93% U^{235} 93.12 wt % ZrH
Hydrogen density, average	6.06×10^{22} atoms/cc
Hydrogen contained in core	378 moles
Diameter of fuel-moderator elements	0.975 in.
Length of fuel-moderator region	10 in.
Total length of fuel elements (1.5 in. long Be plug + 1/2-in. stainless steel on each end of fuel)	14 in.
Fuel cladding	0.010 in. 347 SS
Vitreous coating	0.002 - 0.003 in.
Fuel rod spacing (triangular center to center)	1.015 in.
Diameter of core vessel	9.5 in.
Wall thickness of core vessel	0.094 in.
Core volume	0.35 ft^3
Unit Cell Volume Fractions	
Fuel-moderator material	0.845
Cladding material	0.035
NaK coolant	0.120
Reactor Control	
Reflector	3 in., Be
Number of control drums	3
Control drum worths (at 70 - 135°), average	$2.15
Number of safety elements	3
Safety element worth	$5.40
Control drum insertion rate (maximum)	2.5¢/sec
Safety element insertion rate (maximum)	6¢/sec
Scram time of safety elements	250 msec
Pu-Be startup source (15.78 gm)	1.68×10^6 n/sec
Reactor Physics	
Prompt neutron lifetime	10 μsec
β_{eff}	0.0084
Cold, clean excess reactivity	$9.75
Limited motion of control drums, at 70 - 135°(3)	$5.41
Total control drum worth (3)	$10.95
Total safety element worth (3)	~$13.57
Prompt temperature coefficient (200 - 1000°F)	~ -0.04¢/F°
Overall isothermal temperature coefficient, at 1100°F	~ -0.35¢/F°

TABLE III (Continued)
SER PARAMETERS[1,2,3]

Reactor Physics (Continued)	
Temperature defect (75 - 1100°F)	$3.42
Equilibrium xenon defect	$0.39
Power defect (0 - 50 kw)	$0.23
Ratio of peak-to-average radial flux	1.26
Ratio of peak-to-average axial flux	1.22
Ratio of peak-to-average total flux	1.54
Average power density in core (at 50 kw)	5.45×10^5 Btu/hr-ft^3
Average heat flux in core (at 50 kw)	1.24×10^4 Btu/hr-ft^2
Maximum fuel temperature (at 50 kw and 1200°F outlet NaK temperature)	1270°F
Reactor Cooling System (Design Conditions)	
Coolant, NaK eutectic	78 wt % K
Specific heat of coolant	0.21
Heat capacity of core, fuel, and coolant in fuel section	12.65 kw/sec-°F
Total heat capacity; fuel, coolant, reflector, and structural material	85.7 kw/sec-°F
Reactor outlet temperature (NaK)	1200°F
Reactor inlet temperature (NaK)	1000°F
Coolant inlet temperature to heat exchanger (primary)	1200°F
Coolant outlet temperature from heat exchanger (primary)	1000°F
Coolant inlet temperature to heat exchanger (secondary)	950°F
Coolant outlet temperature from heat exchanger (secondary)	1150°F
Maximum coolant pumping rate (1000°F, 20 psi head)	23 gpm
Type of primary pump	electromagnetic
Diameter of coolant lines in main flow circuits	1-1/4-in.
Capacity of electrical heaters (at 230 v.)	50.4 kw
Maximum auxiliary coolant pump rate (at 70°F and 1 psi head)	0.5 gpm
Diameter of coolant flow lines in auxiliary flow circuit	1/2 in.
Coolant pressure drop across core	< 0.5 in. of H_2O
Cover gas on coolant system	He, primary A, secondary
Primary fill-and-drain tank capacity	24 gal.
Primary surge tank operating pressure	1 psig
Secondary fill-and-drain tank capacity	35 gal.
Secondary surge tank operating pressure	2 psig
Type of secondary pump	electromagnetic
Cover gas on containment vessel and pipe vaults (slightly above atmosphere)	nitrogen
Coolant system design pressure	300 psig

TABLE III (Continued)

SER PARAMETERS[1,2,3]

Reactor Cooling System (Design Conditions) - Continued	
Overall heat transfer coefficient of heat exchanger	818 Btu/hr-ft^2-°F
Type of intermediate heat exchanger	counterflow
Coolant system design temperature	1200°F
Maximum airblast heat exchanger air flow	2500 scfm
Airblast heat exchanger inlet air temperature	100°F
Airblast heat exchanger outlet air temperature	230°F
Airblast heat exchanger damper closing time	6 sec
Maximum airblast heat exchanger fan speed	1725 rpm
Heat load of H_2O cooling system	125,000 Btu/hr
Containment vessel design pressure (tested at 456 psig)	305 psig

III. INSTRUMENTATION AND CONTROL SYSTEM[1]

A. NUCLEAR INSTRUMENTATION

A block diagram of the nuclear instrumentation is shown in Figure 9. This includes appropriate instrumentation for startup-, intermediate-, and power-range operation. The range covered by each neutron chamber used is shown by Figure 10.

Two fission chambers are used to cover the startup range (5×10^{-4} watts to 5 watts). Two compensated ion chambers are used to cover the intermediate range (5×10^{-1} to 5×10^{5} watts). Three uncompensated ion chambers are used with three safety amplifiers to furnish independent high-speed flux level scrams in the power range (5×10^{2} watts to 5×10^{5} watts). An additional channel, consisting of an uncompensated ion chamber and a micro-microammeter, is used to furnish the operator with flux level information.

The neutron chambers are located in 5-in. instrument thimbles outside and adjacent to the containment vessel.

B. PROCESS INSTRUMENTATION

The reactor and auxiliary coolant loops are monitored with temperature, pressure, liquid level, and flow instrumentation. All instruments installed in the containment vessel and primary loop system are capable of withstanding 300 psi. All instrument and control wiring that penetrates the containment vessel is brought out through conduit filled with a resin compound which makes a seal capable of withstanding 300 psi.

C. CONTROL CONSOLE

All major functions of the reactor are controlled from the control console and instrument racks. The instruments are arranged so that the operator can quickly and easily detect faulty operation and apply corrective action.

The nuclear and process instrumentation and recorders are mounted in racks located in front of the control console and are visible to the operator seated at the control console. The controls of immediate interest to the operator are located at the console. These controls include:

1) Control drum drives,
2) Safety element drives,

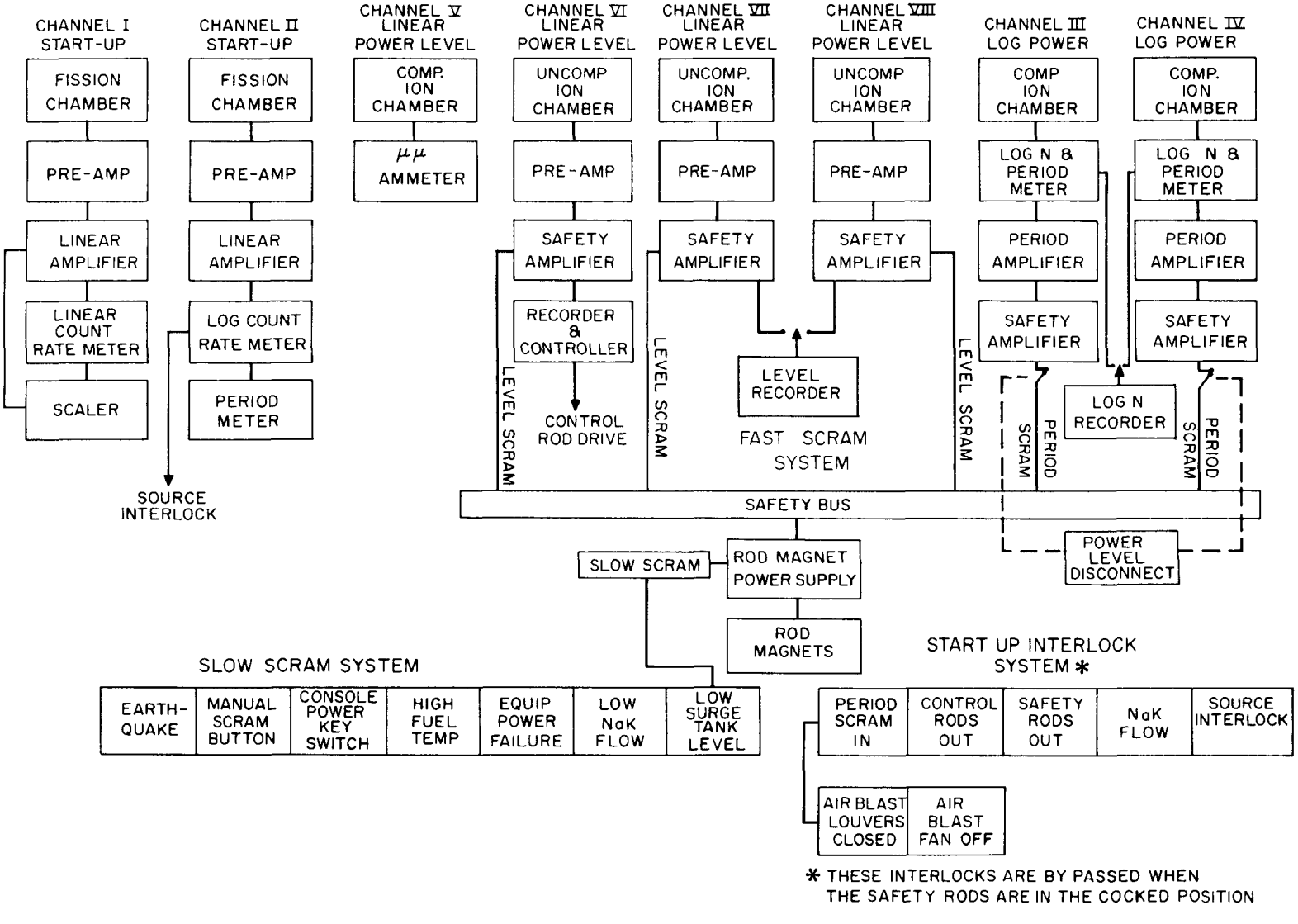

Figure 9. Nuclear Instrumentation

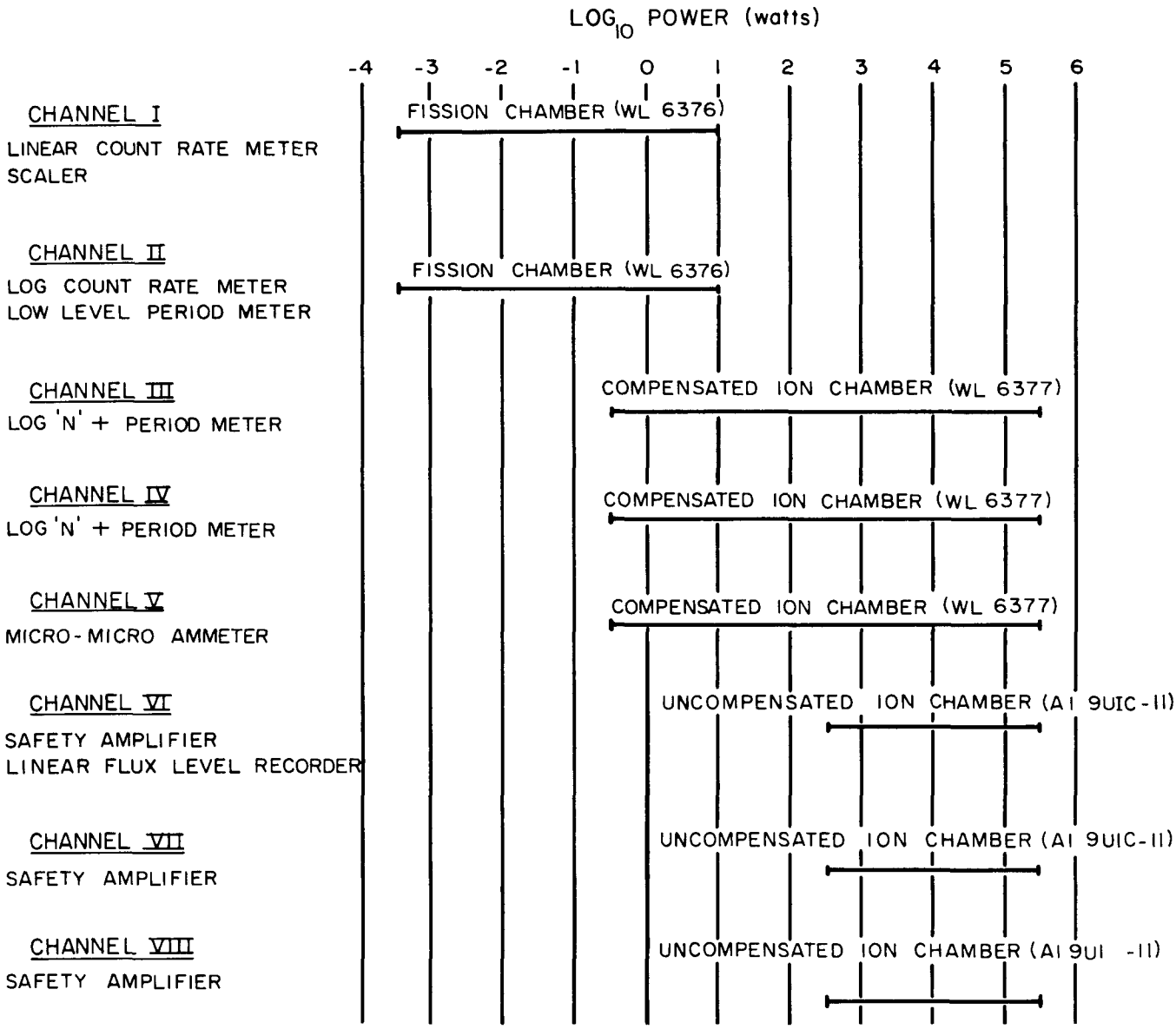

Figure 10. Range of Operation of Neutron Detectors

3) Primary and secondary NaK coolant pump,
4) Manual-to-automatic reactor operation transfer switch
5) Airblast heat exchanger fan, and
6) Emergency scram.

The following meters and indicators are also located at the console:

1) Reactor period,
2) Reactor power level,
3) Control drum position indicator,
4) Safety element position indicator,
5) Primary and secondary NaK flow rate, and
6) Airblast heat exchanger fan speed.

IV. SER OPERATION

A. HIGHLIGHTS OF SER OPERATION

By the middle of September 1959, the SER core was ready to receive the first fuel element. The entire SER complex had satisfactorily completed all functional tests so that the approach-to-dry-critical tests could begin. The first fourteen fuel elements were loaded on September 17, 1959; and dry criticality was attained on September 19 with a core loading of 55 fuel elements. After criticality was achieved, the initial control and safety element calibrations were obtained. The full loading of 61 fuel elements was reached on October 19. On October 20, the reactor was filled with NaK followed by wet criticality on the same date. After a series of tests to determine the operating characteristics of the system, the reactor power and temperature were gradually raised to design level. The reactor was first operated at design conditions on November 9, 1960. Subsequent to the attainment of design operating conditions, an intensive testing program was undertaken to determine the nuclear parameters of the reactor. The results of these tests are presented in Section V.

The first extended power run began on February 22, 1960, and was interrupted on March 12 by an instrument malfunction which resulted in a scram. The second extended power run was begun the same day and continued until April 23 when the reactor was manually shut down after attaining 1000 hr of continuous operation at design power and temperature.

From this time until November 1960, the reactor was operated in accordance with the requirements of the various tests that were being conducted. As of November 19, 1960, 224,650 kw hr of thermal energy had been generated by the SER. A total of 1877 hr was logged at design conditions of 50 kw and 1200°F outlet temperature. Figure 11 shows the relationship of energy generated to average core temperature.

Figure 12 is a bar graph showing the salient points of reactor operation until final shutdown on November 19, 1960.

A summary of the SER operation is given in Table IV.

A number of scrams has occurred since the SER has been in operation. The number of occurrences and probable cause are listed in Table V in their order of frequency.

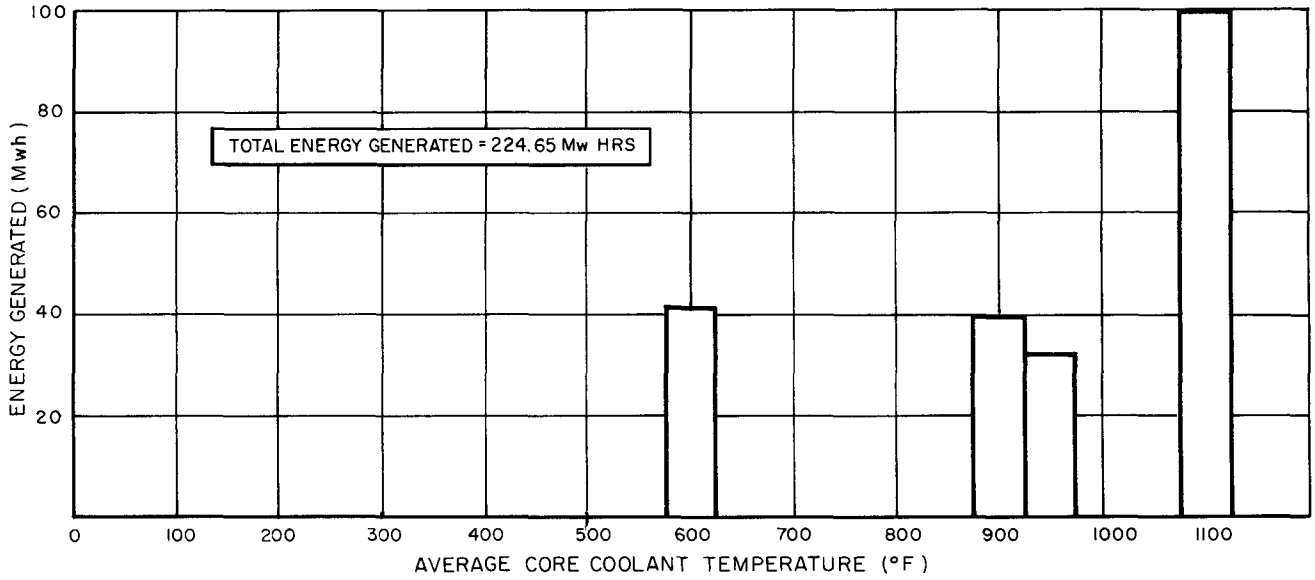

Figure 11. SER Operation at Various Core Coolant Temperatures

TABLE IV

SUMMARY OF SER OPERATION

Initial fuel loading	September 17, 1959
Final shutdown	November 19, 1960
Elapsed time during testing	10,306 hr, 440 days
Reactor operating time	6,035 hr, 58.5% of total time
Operation at 50 kw and 1200°F core outlet temperatures	1877 hr, 31.1% of total operating time
Operation at 50 kw and less than 1200°F core outlet temperature	2,290 hr, 38.0% of total operating time
Operation less than 50 kw and less than 1200°F core outlet temperature	1,868 hr, 30.9% of total operating time
Reactor down time	4,271 hr, 41.5% of total time
Holidays and weekends	1,288 hr, 30.1% of total down time
Routine maintenance and experimental preparation	1,245 hr, 29.2% of total down time
Heater bundle failure	680 hr, 15.9% of total down time
Other component failure	1,058 hr, 24.8% of total down time
Total energy generated	224.6 megawatt hr
Equivalent time at 50 kw	4,493 hr $\approx$ 187 days

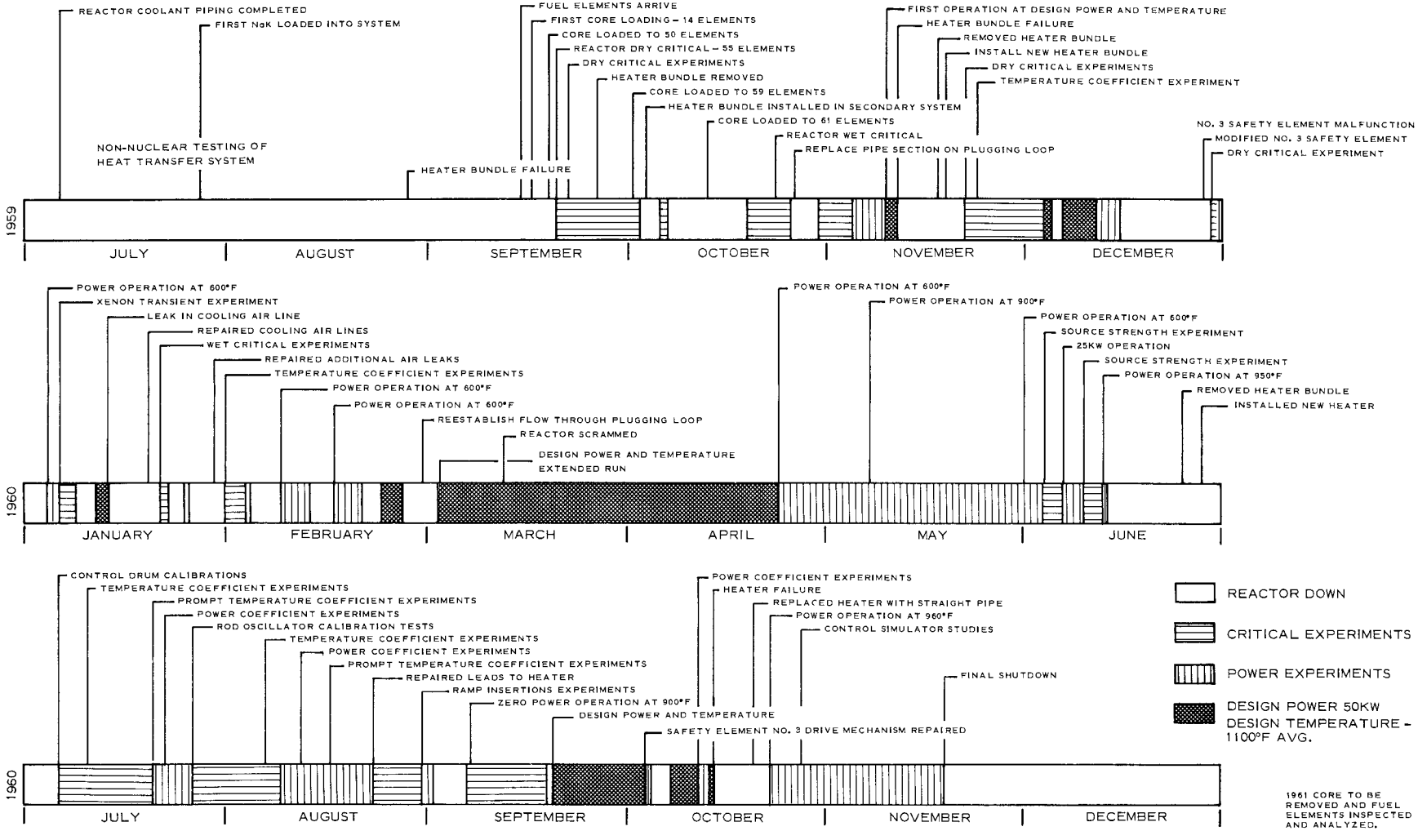

Figure 12. SER History

TABLE V

SCRAMS

Number of Occurrences	Probable Cause
17	Abnormal signal in log power channels 3 and 4 and power level channels 5 through 8
15	Individual safety dropped out
13	Low J-tube NaK level alaram
12	Circuit noise and accidental
6	False signal, source unknown
3	Disturbing instrument cable in trench
3	Low level period
1	Instrument trouble
1	Heater bundle failure
1	Power failure
0	Initiated internal to core
72	Total through August 31, 1960

B. MAINTENANCE PROBLEMS

1. Process

Considerable operating experience with liquid-metal cooling loops had been gained from the design, construction, and operation of liquid-metal-cooled reactors such as the Sodium Reactor Experiment (SRE); thus, no major problems have been encountered in the process system of the SER. Most of the problems have been of a minor nature and have not resulted in any major modification to the system.

The factor causing the most scrams was "abnormal signal in log power channels 3 and 4 and power level channels 6 through 8." The majority of these scrams were caused by the transient signals introduced into channels 3 and 4 when the period protection circuitry was switched into the safety circuitry. The period protection circuitry is normally removed from the safety circuitry with an on-off switch when the reactor is at full power. The period protection circuitry must be switched in when the reactor power is dropped below 10 kw. This switching nearly always causes a scram.

Malfunction of period channel No. 3 caused several scrams at periods as long as 30 sec. Normally, a scram should not be initiated by the safety instrumentation until a 3-sec period exists. Channel No. 3 instrumentation was subsequently repaired. A scram was initiated from power channel No. 7, because the scram point for this channel was set too low. The normal scram point is 75 kw.

Fifteen scrams occurred because an individual safety dropped out. This usually occurred during a rise in temperature of the reactor, and would indicate that the expansion of the different components of the safeties and the core vessel may have forced the safety to pull away from the magnet. The tension of the springs on the safety drives was adjusted several times in an attempt to remedy this situation.

Scrams caused by the J-tube NaK level alarm were usually due to spurious signals in the J-tube circuitry. The instrument measures a voltage of only about 10 mv ac and noise pickup presented a difficult problem. Modification and maintenance was only partially successful in eliminating this noise. Several J-tube scrams were initiated by surges in the power line.

Circuit noise in the low level period meter also contributed to the scrams. No scrams occurred because of a short reactor period. All period scrams were caused either by instrument malfunction or by noise in the circuitry; i.e., no scrams were due to abnormal condition within the core.

Accidental scrams were due to someone accidentally bumping an instrument such as the J-tube meter.

One scram was attributed to instrument trouble. This means that a component in each of two of the three power safety channels was malfunctioning simultaneously.

Heater bundle failure caused two scrams. The magnitude of the leaks was not sufficient to cause scrams from low NaK level indication, but was caused by electrical shorts in the primary vault components due to the presence of NaK vapor.

An immersion type electric heater used to heat the NaK coolant was originally installed in the primary loop. However, a heater bundle failure which occurred in August 1959, prior to reactor operation, pointed out the possibility

of leaking radioactive NaK into the vault, should the heater bundle fail during reactor operation. Primarily for this reason, the heater bundle was removed from the primary system and was installed in the secondary loop. One of the reasons for failure of the primary loop heater bundle was the lack of adequate interlocks that would automatically turn off the heater on loss of coolant flow. Consequently, during pre-startup testing of the primary NaK loop, the primary pump was stopped without cutting off the power to the heater. This caused the NaK to boil and over-stressed the calrod heaters, which resulted in a NaK leak.

Three different heater bundles have been installed in the secondary NaK loop. The first, which was similar in design to the original primary heater, failed after only a few months of operation and was replaced in late November 1959, by one of external design; i. e., the calrod heaters were external to the piping. Trouble-free operation was obtained with this heater until March 1960, when the first calrod failed. Continued difficulties were encountered until this heater was replaced in June. The third heater bundle for the secondary loop was of the immersion type; of a different design than that of the original heater. Until the end of August 1960, no further difficulties with heater bundles have been experienced.

Other minor problems that affected reactor operations were: (a) leaks in the air-cooling system of the shutdown shield which caused a pressure rise in the reactor containment vessel; and, (b) a failure of the airblast heat exchanger fan.

Although these problems resulted in an interruption in reactor operation, no difficulty was experienced in accomplishing the necessary repairs.

2. Instrumentation and Control Problems

Component failure in the nuclear and process instrumentation has been quite small. During the 1000-hr operation at design power and temperature, the only failure in the instrumentation was in one of the intermediate power level channels used for period protection at power levels below 10 kw. Consequently, during power operation this did not necessitate a shutdown for repair.

During reactor startup, some instrumentation problems were encountered. The most troublesome was noise in the startup pulse channels. Most of the difficulty was the result of placing the low-level pulse wiring and the control wiring

in a common trench. By placing the low-level pulse wiring in a shielded, flexible tubing this condition was alleviated but not entirely solved.

Numerous scrams were caused by spurious NaK level signals resulting from the telemetering lines being in close proximity to control power wires. The voltage level coming into the control room is in the order of 15 mv. Any spurious noise from switching and relay contacts was easily picked up by the NaK level circuit. Also, fluctuations in power line voltage affected the circuit. This problem has not been entirely solved.

Thermocouple failures were numerous, pointing out the need for better materials and for improved installation methods. The resistance thermometers on the inlet and outlet NaK piping below the shutdown shield failed soon after reactor startup. Since they were located in an inaccessible spot, it was necessary to rely on thermocouples external to the shutdown shield for inlet and outlet NaK temperature data. The in-fuel thermocouples exhibited a wide variation in output indicating as much as 200°F difference in some instances. This required that they be periodically calibrated to ensure no additional drift.

The high ambient temperature of the primary vault damaged the insulation on the heater wiring for the plugging meter, which resulted in numerous failures. The installation of high-temperature heater wire resolved this problem.

The automatic control system was designed as a temperature controller; however, early failure of the differential thermocouples on the core in-and-out piping resulted in the system's being modified so that the power level could automatically be controlled by the neutron flux.

The flowmeter for the primary NaK loop was installed in such a way that the entire NaK flow passes through it. However, a small amount of flow bypasses the reactor core to the plugging meter. Consequently, the flowmeter indicates a slightly high flow rate for the core. It was not practical to change the location of the primary flowmeter on the SER, but further installations should keep this in mind.

The nuclear and process instrumentation, as a whole, has functioned very well with very little modification to the original equipment.

V. SER TESTS

The objectives of the SER tests were to investigate reactor characteristics: (a) the ability of the reactor to override the reactivity losses associated with obtaining operating conditions and extended operation at these conditions, and (b) the stability and safety of the reactor.

A. REACTIVITY OVERRIDE TESTS

To determine the ability of the reactor to override reactivity losses associated with operation it was necessary to measure the following parameters:

1) The cold, clean, excess reactivity;
2) The worth of the control elements;
3) The temperature defect, cold-to-hot;
4) The power defect, zero power to 50 kw;
5) The defect associated with equilibrium xenon; and
6) The long-term reactivity losses.

B. STABILITY AND SAFETY TESTS

To determine the stability and safety of the reactor it was necessary to measure these additional reactor parameters:

1) The worth of the safety elements,
2) The time associated with the safety element action for reactivity removal, and
3) The temperature coefficients of the reactor.

The measurement of these parameters is detailed and summarized.

C. THE COLD, CLEAN, EXCESS REACTIVITY

The determination of the cold, clean, excess reactivity was made during the initial loading of the reactor with fuel. Dry criticality was achieved with a loading of 55 fuel elements. Zero power control-element and safety-element worth determinations took place concurrently during the loading of the core so that the values of the fuel-moderator-element worth could be found. Figure 13 presents a plot of the excess reactivity vs number of fuel elements loaded. The shape of the curve indicates that the reactivity worth of each fuel element increases per fuel element added. Note that the fuel loaded into the flats of the

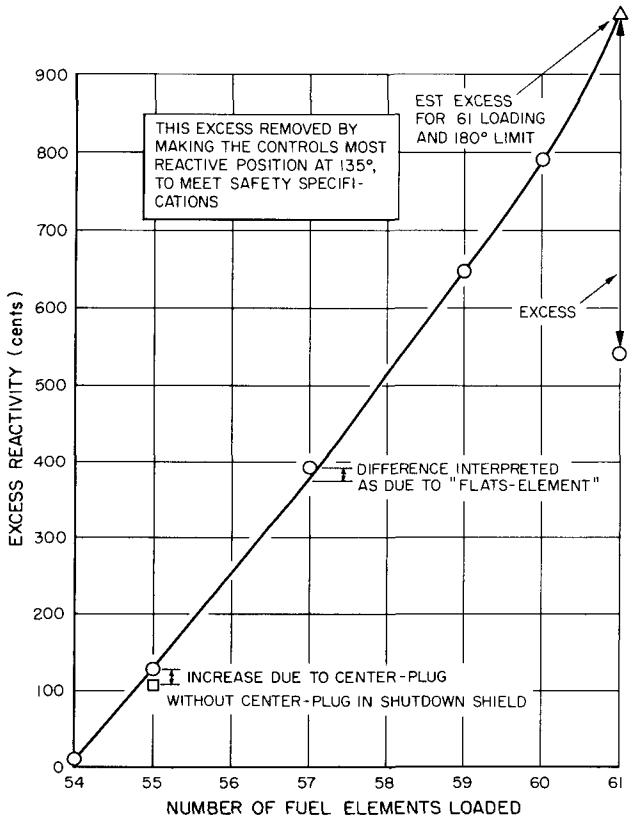

Figure 13. Excess Reactivities for Various Fuel Loadings

hexagon-shaped core has a greater worth than fuel loaded into the corners. This result shows that the closer radius of a "flat" element has considerable effect on the element worth. Figure 13 also shows the increase reactivity resulting from the insertion of the center plug into the shutdown shield.

The removal of a fuel element next to control drum No. 2 during the 60-element loading caused a pronounced reduction (by about 14%) in the worth of the control drum. Similar effects were noted for other cases where fuel elements were missing near a control drum or safety element.

During the final fuel loading, a stainless steel dummy was inserted into the outer corner of the core lattice in place of a fuel-moderator element. This resulted in an increase in reactivity of approximately 17¢. This increase in reactivity is attributed to the increase in reflective property of the stainless steel dummy.

Before the addition of the 61st element, the inward rotation of the control drums was limited to 135° to comply with the SER Hazards Report specification of a 4% excess.[1] Thus, the excess reactivity available to the reactor operator for the 61-element loading was $5.41; whereas, $9.78 would have been available were the control drums allowed a full 180° rotation.

After the determination of the cold, clean, excess for a NaK-free core, a measurement was made of the change in reactivity associated with the addition of the coolant. The results from this test and from subsequent tests made throughout the core life indicated that this addition caused reactivity losses of the order of 5¢. This small net loss in reactivity is probably due to the positive reflector effect in the outer core regions cancelling the poisoning effect of adding NaK to the central region of the core.

The change in reactivity due to changes in fuel content and hydrogen content have been theoretically determined but have not been checked experimentally. These ratios are:

$$(\Delta k/k)/(\Delta N_u/N_u) \cong 0.064,$$

and

$$(\Delta k/k)/(\Delta N_H/N_H) \cong 0.46.$$

D. WORTH OF THE CONTROL ELEMENTS

During the initial loading of the reactor and at intervals during the operation of the reactor, measurements were made of the worths of the control drums. All of these measurements used the technique of making small motions of the control elements to place the reactor on a measureable, supercritical period. This period was interpreted through the in-hour relationship (using a $\beta = 0.0084$) to give the change in reactivity associated with the control element motion. The total worth of a control element was taken to be the summation of such determinations over the total span of the drum rotation. This assumption seems to be valid due to the fact that there has been no evidence of interaction between the control elements.

Table VI gives the total worth of the control elements measured during the initial loading buildup. The reported worths for those loadings of less than 61 elements are for the full 70 to 180° rotation of the element. The region of the drums from 0 to 70° was not used, due to the low worth, $\sim 17¢$.

A determination of the worth of control element No. 3 was made immediately after the addition of coolant to the reactor and before any power production by the reactor. The total worth (over 70 to 135° rotation) of this control element was $2.25.

The drums were again calibrated after 5932 kwh energy release. For a period of 12 days prior to the calibrations, the reactor had generated no power. The worth of the control elements is given in Table VII for various core average temperatures.

The drums were again recalibrated after 147,358 kwh energy release by the core. For a period of 35 days prior to the calibrations, the reactor had been at zero power. The worth curves established at this time for two different

TABLE VI

TOTAL CONTROL ELEMENT WORTHS, DRY CORE

Fuel Loading (Number of Elements)	Control Worths (cents) (at 70 - 180° rotation)		
	1	2	3
54	-	-	173
55	-	263	257
57	-	-	336
59	-	-	336
60 + 1 dummy	340	297	349
	Control motion limited to 135°		
61	-	-	230

TABLE VII

CONTROL ELEMENT WORTHS, WET CORE
(5932 kwh Energy Release)

Control Element Number	Control Element Worth (cents) (at 70 - 135° rotation)		% Difference
	at 268°F	at 584°F	
1	216	218	+0.92
2	230	228	-0.87
3	230	228	-0.87

temperatures, together with those obtained in November 1959, are presented in Figures 14, 15, and 16, and the total worths are presented in Table VIII.

A comparison of the tabulated values of the control drum worths indicates that there is no drastic temperature dependence and that the addition of coolant to the reactor does not affect the worths. There is an unexplained difference between those calibrations conducted during initial operations and those conducted after large amounts of power generation. There is no reason to assume that either of these calibrations is more valid than the other without knowing the cause for the difference in calibration. It is hoped that additional control drum calibrations to be performed after the release of more energy from the core will permit a meaningful interpretation of this variation. However, if it is assumed that there is no change in drum calibration with temperature, the percent difference listed in Tables VII and VIII is an indication of the accuracy of the measurements.

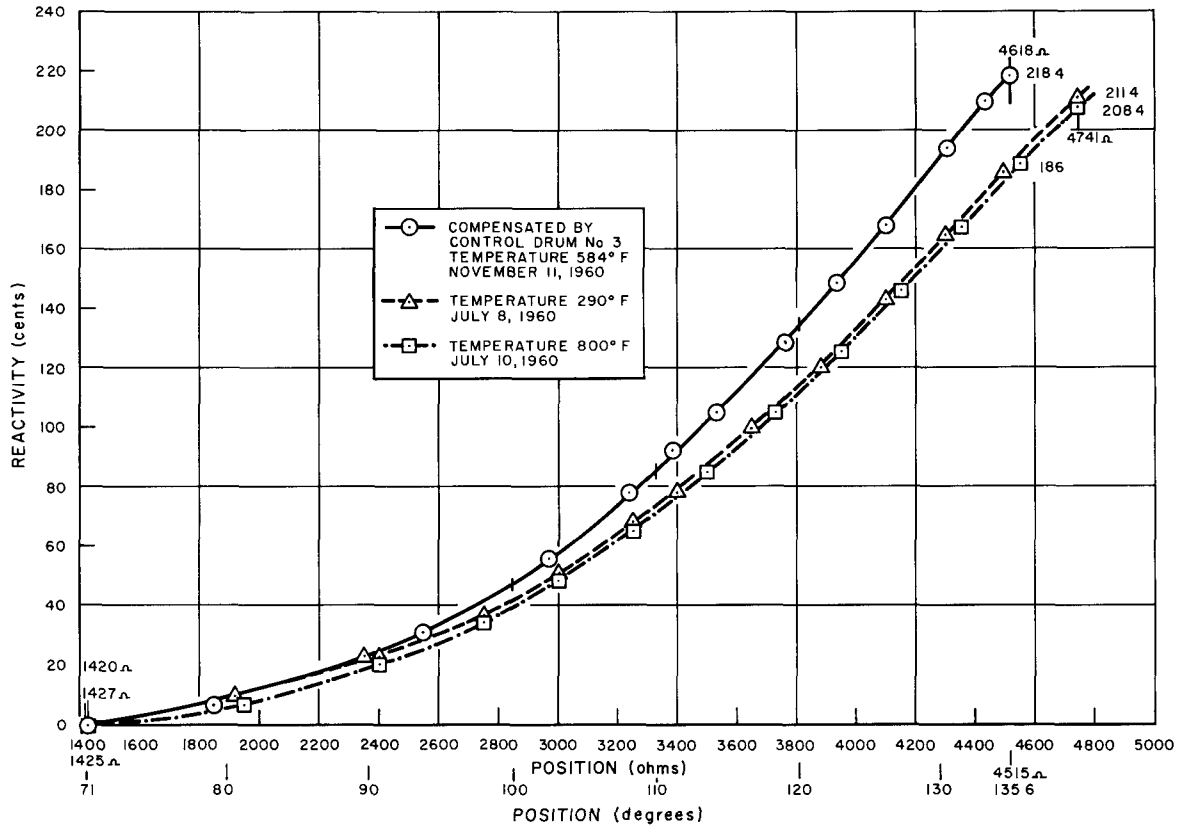

Figure 14. Control Drum No. 1, Comparison of Drum Worths After 141,100 kwh of Operation

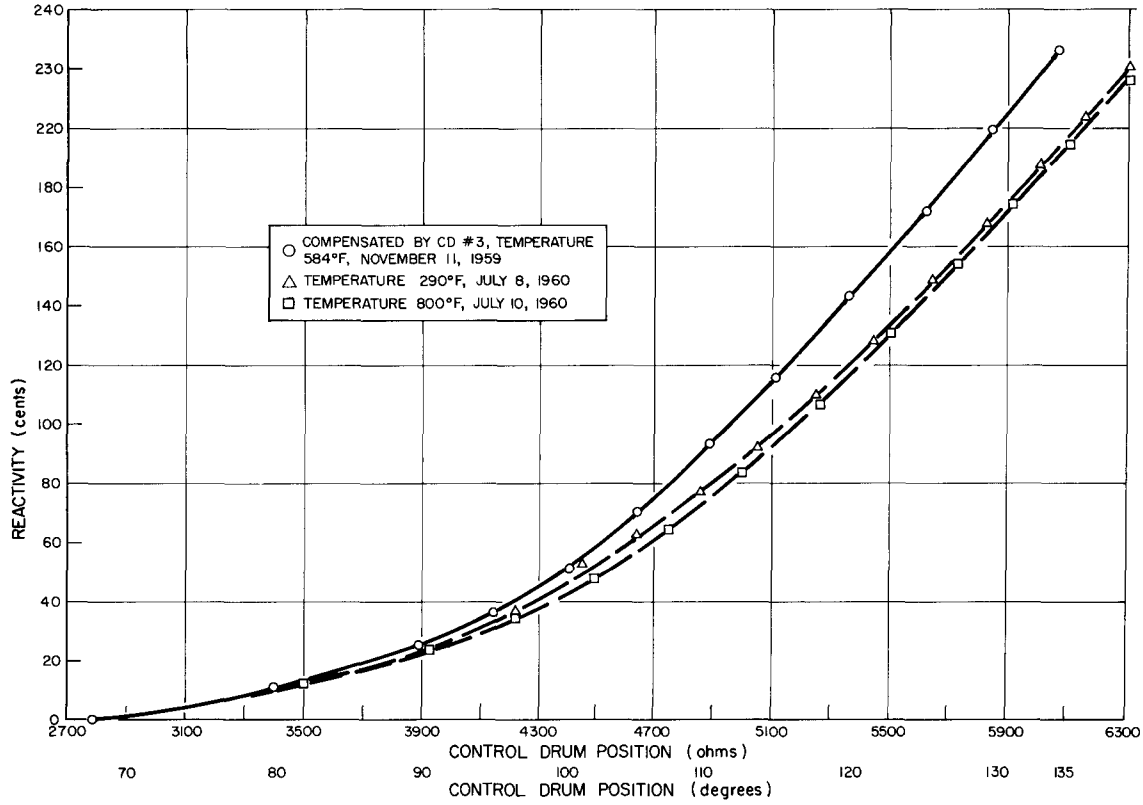

Figure 15. Control Drum No. 2, Comparison of Drum Worths After 141,100 kwh of Operation

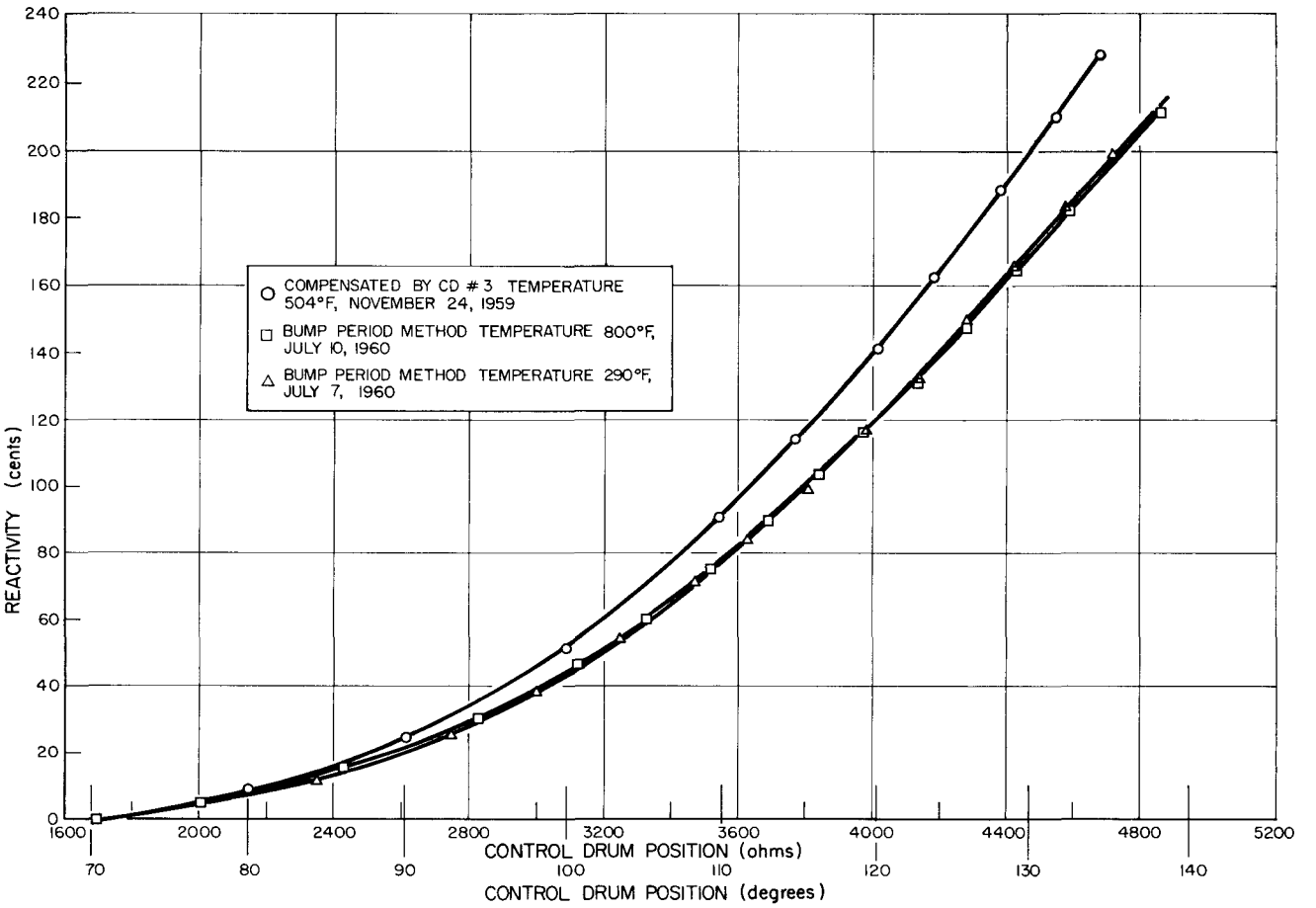

Figure 16. Control Drum No. 3, Comparison of Drum Worths After 141,100 kwh of Operation

TABLE VIII

CONTROL ELEMENT WORTHS, WET CORE
(147,358 kwh Energy Release)

Control Element Number	Control Element Worth (cents) (at 70 - 135° rotation)		% Difference
	at 290°F	at 800°F	
1	211	209	-0.95
2	221	217	-1.81
3	217	215	-0.92

For the purposes of this report, all measurements dependent on control drum calibration will refer to those sets used in the interpretation as either the earlier or later set; thus, differentiation is made between those calibrations done prior to the release of large amounts of energy and those done after the release.

E. THE TEMPERATURE DEFECT

The temperature defect of the SER was determined by heating the reactor with external heat to approximately 600°F, then bringing the reactor to 50 kwt power, and heating to the design average core temperature of 1100°F. The positions of the control drums were recorded throughout this process and reactivity changes were correlated with changes in temperature by the use of the earlier control drum calibrations. The plot of change in reactivity with temperature is presented in Figure 17. A normalization has been performed to remove the effects of xenon buildup and the power defect from that portion of the curve above 600°F. Over the linear portion of this curve $d\rho/dT = 0.4¢/F°$.

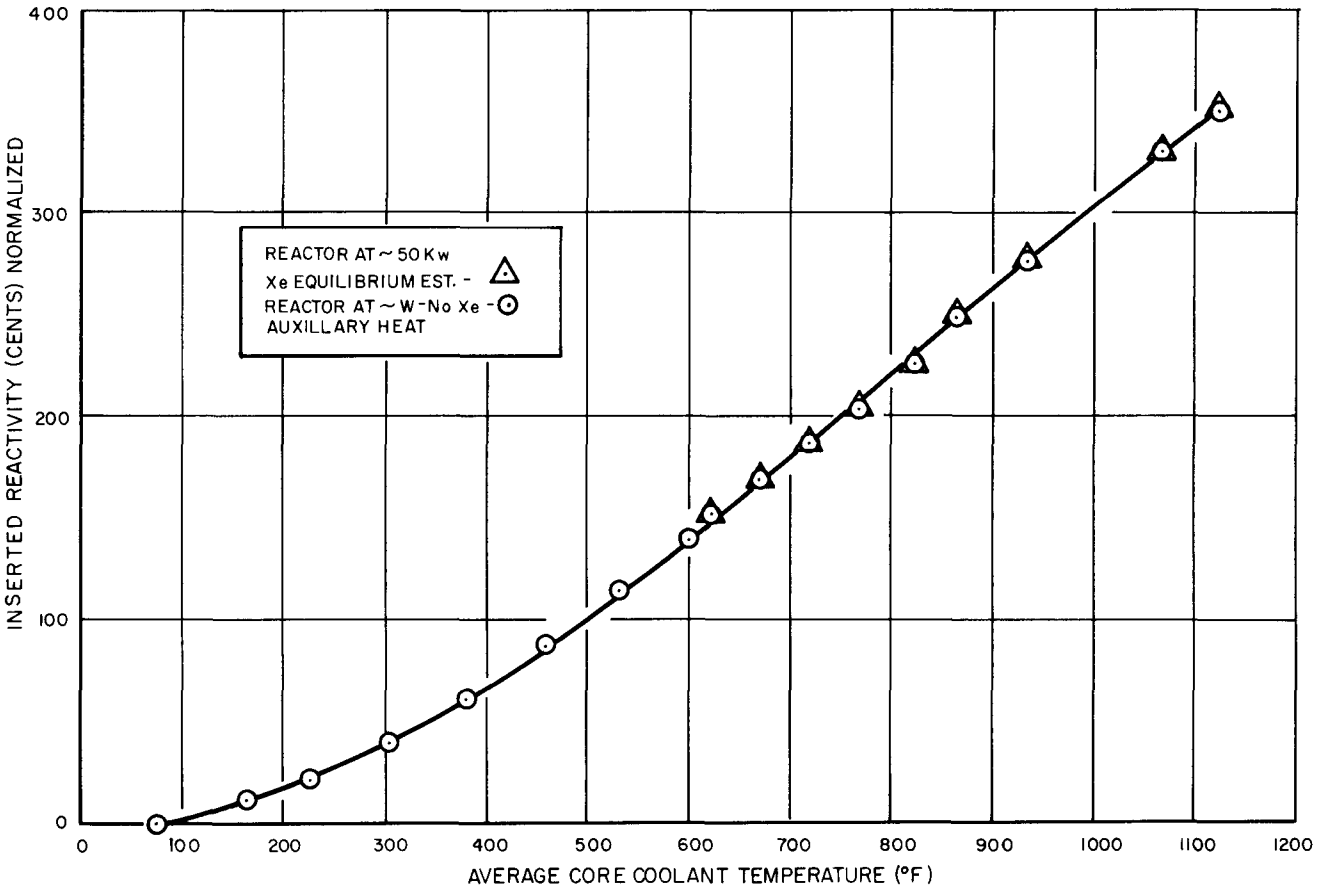

Figure 17. SER Data, Temperature Defect From Data of Experiments for December 19, 1959

F. THE POWER DEFECT

The change in reactivity with power in the SER is ascribed to the establishment of temperature gradients throughout the core. A more detailed discussion of the effect of these gradients will be presented in the discussion of temperature

coefficients. The measured reactivity loss associated with the change from zero power to 50 kw was found to be 23¢ by the interpretation of the drum motion associated with this change and by use of the earlier control drum calibrations.

G. EQUILIBRIUM XENON DEFECT

The observation of control drum motion during the establishment of equilibrium xenon indicates an equilibrium xenon defect of 39¢. There is no peaking of the xenon concentration after reactor shutdown due to the low flux density of the reactor. A comparison of the calculated xenon transient and the measured xenon transient is presented in Figure 18. It is seen that these two curves are in close agreement.

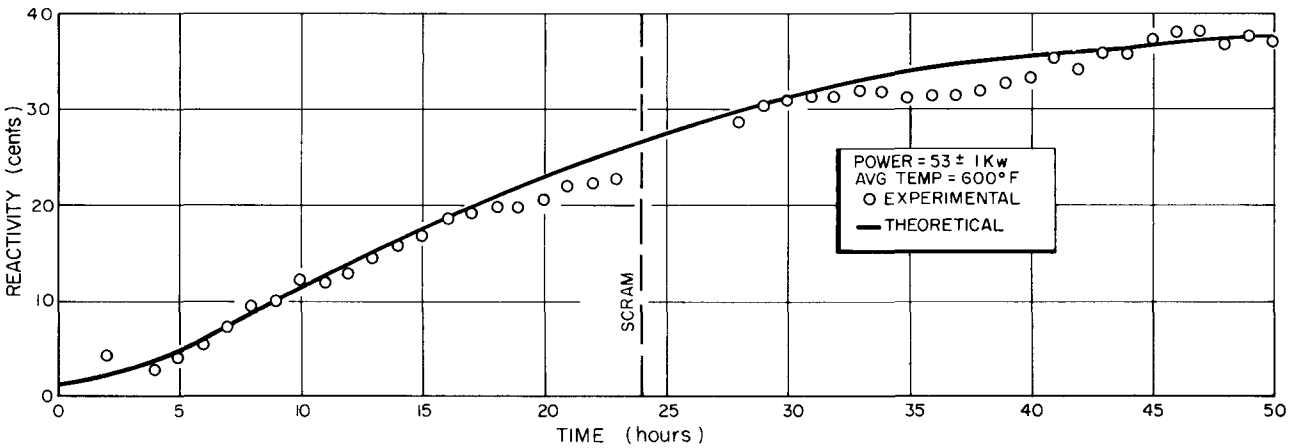

Figure 18. SER Xenon Transient Experiment

H. LONG-TERM LOSS RATE

The long-term losses associated with the operation of the SER are both power and temperature dependent. The power dependent losses are attributed to fuel burnup, samarium buildup, and fission product poisoning other than samarium or xenon. Of these, the buildup of samarium is calculated to be the largest factor. The temperature dependent losses are attributed to the loss of hydrogen from the fuel-moderator rod. This phenomenon would take place due to dissociation of hydrogen from the matrix material and its subsequent diffusion through the element cladding. Long-term runs at 50 kw were accomplished at core outlet temperatures of 1200, 1000, and 700°F; and the reactivity loss rates were determined from the motion of the control drums during these runs. The

drum calibrations used to determine these loss rates were the later calibrations. The loss rates measured during these runs are presented in Table IX and in Figure 19.

TABLE IX

LOSS RATES

Core Average Temperature (°F)	Reactivity Loss Rate (¢/day)
1100	0.79 ± 0.03
900	0.39 ± 0.02
600	0.26 ± 0.04

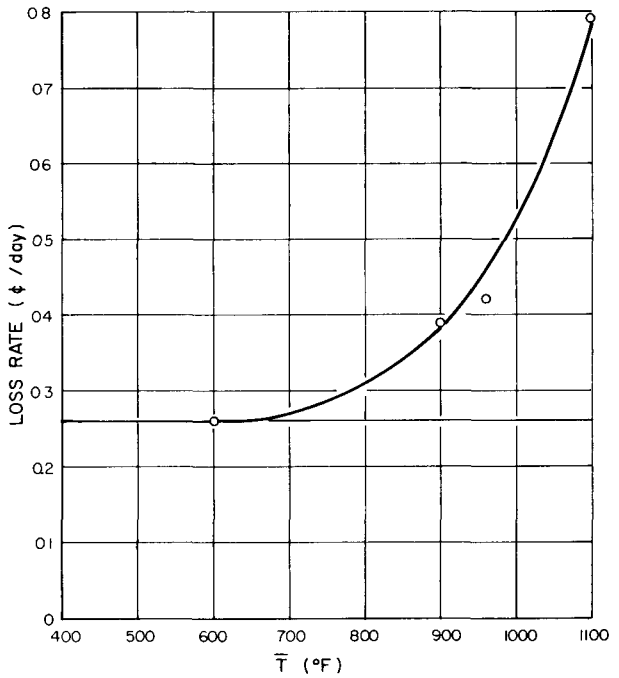

Figure 19. Measured Loss Rate vs Average Core Temperature

The assumption is made that the temperatures involved in the 700°F outlet case are low enough for the loss of hydrogen to be negligible. The 0.26¢/day loss rate is interpreted as due to samarium and longlife fission product poisoning plus fuel depletion from operation at 50 kw. The difference between this value and the loss rates established at the more elevated temperatures may be associated with the loss of hydrogen at those temperatures.

I. SUMMARY OF PARAMETERS PERTINENT TO THE OVERRIDE OF REACTIVITY LOSSES

Cold, clean, excess reactivity	
Drum rotation to 180°	$9.78
Drum rotation to 135°	$5.41
Control Worth, total (old calibration)	
Drum rotation to 135°	$6.77
Temperature Defect	
75 - 1100°F core average temperature	$3.42
Power Defect	
Zero kw to 50 kw at 600°F	$0.23
Xenon Defect	
Equilibrium at 50 kw	$0.39
Reactivity Loss Rates	
50 kw, 1200°F core outlet	0.79¢/day
50 kw, 1000°F core outlet	0.39¢/day
50 kw, 700°F core outlet	0.26¢/day

J. SAFETY ELEMENT WORTHS

The worths of the SER safety elements were determined during the initial critical measurements. The technique used was to compensate for an outward motion of a safety element by the inward rotation of a control drum and to rely on the calibration of the control drum to associated a reactivity change with the motion of the safety element. This technique required that some use be made of control drums adjacent to the displaced safety element. Interaction between adjacent control and safety elements would be expected. Therefore, the values quoted for the worth of the safety elements can only be used as being indicative of their worth, and not as an absolute determination. The values thus obtained for the total reactivity worth of each safety element are:

Safety Element Number	Total Worth (dollars)
1	$4.60
2	$4.60
3	$4.40

A typical safety element worth curve is shown in Figure 20.

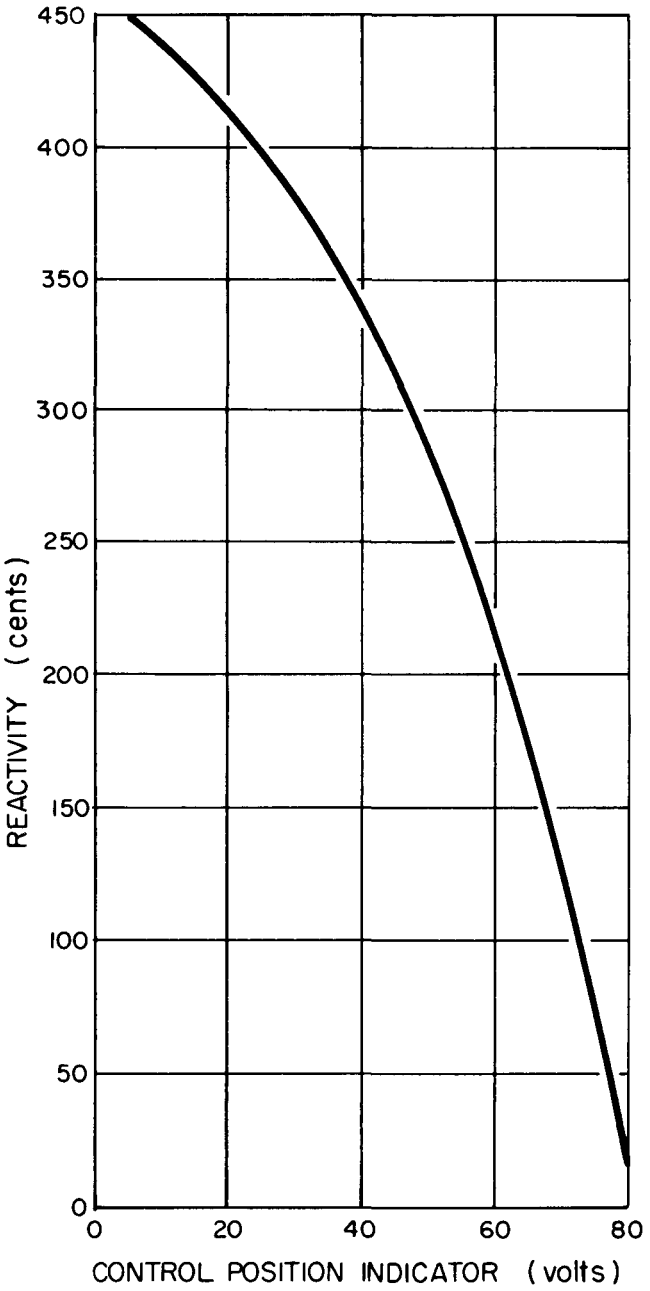

Figure 20. Typical Safety Element Worth Curve

K. SAFETY ELEMENT DROP TIMES

The drop time of the safety elements has been measured at intervals during the operation of the SER. The technique used to make these measurements consisted of photographing cathode ray tube displays of the time variation of the voltage from a potentiometer driven by the safety element. The drop times have been consistent throughout the history of the reactor. These times are approximately 250 msec from initiation of the drop signal until contact is made with the shock absorber. Recoil of the safety elements from the shock absorbers is slight.

L. TEMPERATURE COEFFICIENTS

The stability and safety of operation of the SER is determined mainly by the sign and magnitude of its reactivity responses to temperature changes. Because of the importance of these phenomena, a large portion of the testing on the SER was devoted to a study of temperature effects. Studies were conducted not only to determine the temperature response at the design conditions, but over a spectrum of temperatures, so that information could be obtained to check calculational techniques. The overall temperature response may be considered to be the sum of several effects.

One portion of the temperature response should be that associated with changes in temperature of the fuel-moderator material. Due to the intimate contact of the fuel and moderator, a prompt, negative coefficient is associated

with these elements. The only time-delay from changes in power to action of this coefficient are associated with the thermal capacity of the elements themselves. This thermal capacity has been reported to vary from 14 kw-sec/F° at 200°F to 20 kw-sec/F° at 1000°F.

Another portion of the temperature response of the reactor is referred to as the grid plate temperature coefficients. Changes in the temperature of the plates in which the ends of the fuel are constrained would change the geometry of the reactor, thereby varying the reactivity. The reactivity response through this coefficient to changes in reactor power would have a longer time constant than that of the fuel coefficient due to: (1) the delay time associated with the passage of heat through the fuel element cladding, then the coolant, to the grid plates, and (2) due to the thermal capacities of the plates themselves.

Additional effects on reactivity by temperature may be associated with those slower acting changes which are related to the heating of the core vessel and safety elements, and which change the reflector properties.

By use of these discussions as the definition of three temperature coefficients (a_f, the coefficient associated with the change in temperature of the fuel-moderator elements; a_g, the coefficient associated with the change in core geometry due to grid plate motion; and a_r, the coefficient associated with change in reflector properties) one may write the following equation:

$$\frac{d\rho}{d\overline{T}} = a_f \frac{dT_f}{d\overline{T}} + a_{g1} \frac{dT_{g1}}{d\overline{T}} + a_{g2} \frac{dT_{g2}}{d\overline{T}} + a_r \frac{dT_r}{d\overline{T}}$$

Where $\overline{T}$ is any reference temperature usually taken to be the average core temperature; and T_f, T_{g1}, T_{g2}, and T_r are the temperatures of the fuel elements, lower grid plate, upper grid plate, and reflector, respectively.

To investigate these temperature responses, a series of tests was conducted on the SER These are detailed below:

1. Isothermal Temperature Coefficient

The most straightforward determination of the temperature coefficients associated with the SER is the measurement of the coefficient under isothermal conditions. In this case, the statement:

$$\frac{d\rho}{d\overline{T}} = a_f \frac{d\overline{T}_f}{d\overline{T}} + a_{g1} \frac{d\overline{T}_{g1}}{d\overline{T}} + a_{g2} \frac{d\overline{T}_{g2}}{d\overline{T}} + a_r \frac{d\overline{T}_r}{d\overline{T}}$$

would reduce to:

$$\frac{d\rho}{d\overline{T}} = a_f + a_{g1} + a_{g2} + a_r$$

The closest approach to isothermal conditions possible on the SER is that condition under which no power is produced by the core and any temperature changes are produced by heating the coolant external to the reactor. Measurements, under these conditions, were accomplished in the temperature range 150 to 925°F. The limitations on the capacity of the external heater precluded higher temperature determinations.

To minimize the errors normally associated with differential measurements, extreme care was used in this test. Whenever possible, control drum motion was limited to one drum, to minimize positioning uncertainty. The reactor was stabilized at a temperature, and several reactor periods were measured with the positions of the controlling drum noted for each period measured. The temperature of the reactor was then changed and stabilized at a new temperature. The controlling drum was then returned to the positions at which periods were determined at the previous temperature, and periods for these positions determined. In this manner, difference in reactivity could be implied from the direct comparison of two periods measured with all reactor parameters the same, except for the reactor temperature. Thus, the temperature coefficient, $\Delta\rho/\Delta T$, was determined for temperature steps of approximately 40°F, and no reliance had to be placed on previously measured control drum calibrations. The results of this series of measurements are presented in Figure 21.

From this measurement, the overall temperature coefficient seems to be smoothly varying, almost a linear function of temperature, and a value of approximately -0.35¢/F° may be extrapolated for a core average temperature of 1100°F.

2. Power Coefficients

One method which may be used to attempt to separate the measured overall temperature coefficient into its various components is to measure the variation

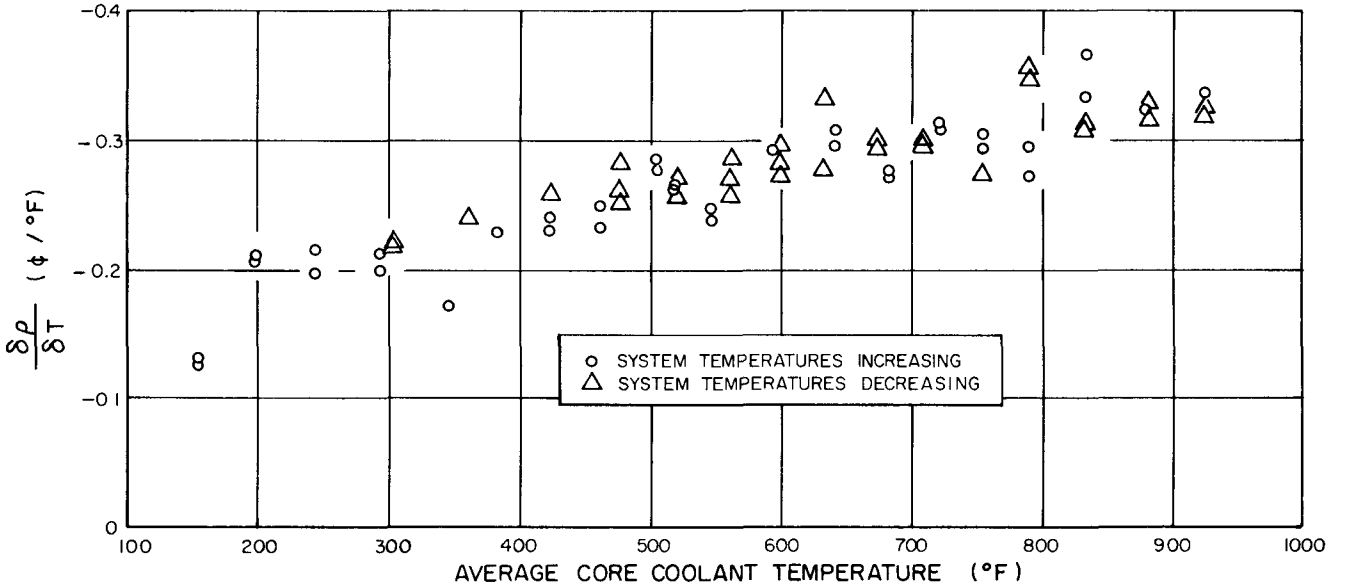

Figure 21. Temperature Coefficient ($\Delta\rho/\Delta T$) vs Average Core Coolant Temperature

in reactivity with reactor power under carefully controlled conditions. The measured "power coefficient" may be expressed:

$$\frac{d\rho}{dp} = \frac{\partial\rho}{\partial T_f}\frac{dT_f}{dp} + \frac{\partial p}{\partial T_{g1}}\frac{dT_{g1}}{dp} + \frac{\partial\rho}{\partial T_{g2}}\frac{dT_{g2}}{dp} + \frac{\partial\rho}{\partial T_r}\frac{dT_r}{dp}$$

It can be seen that, if the power coefficient is measured in such a way that the gross core temperatures are unaffected, the terms

$$\frac{dT_{g1}}{dp}, \frac{dT_{g2}}{dp}, \text{ and } \frac{dT_r}{dp} \text{ would go to zero and } \frac{d\rho}{dp} = \frac{\partial\rho}{\partial T_f}\frac{dT_f}{dp} \text{ constant}$$

T_{in}, T_{out}.

A series of power coefficient studies were made under conditions of constant coolant outlet and inlet temperature. This was accomplished by varying the flow. One of the underlying assumptions of this study is that the flow distribution, and thus the temperature profile, are unaffected by such flow changes.

The results of these studies for varying core average temperatures are given in Figures 22 and 23. Studies have shown that the quantity dT_f/dp is

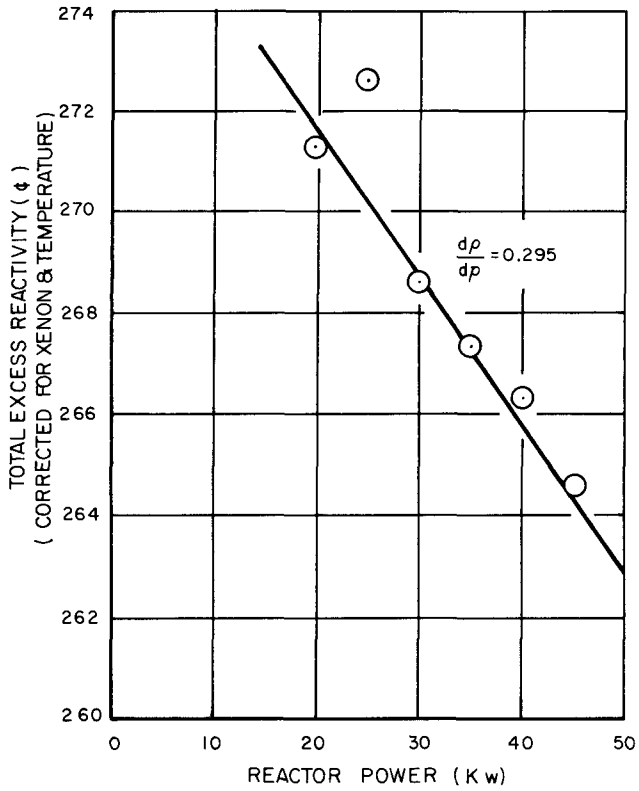

Figure 22. SER Power Coefficient

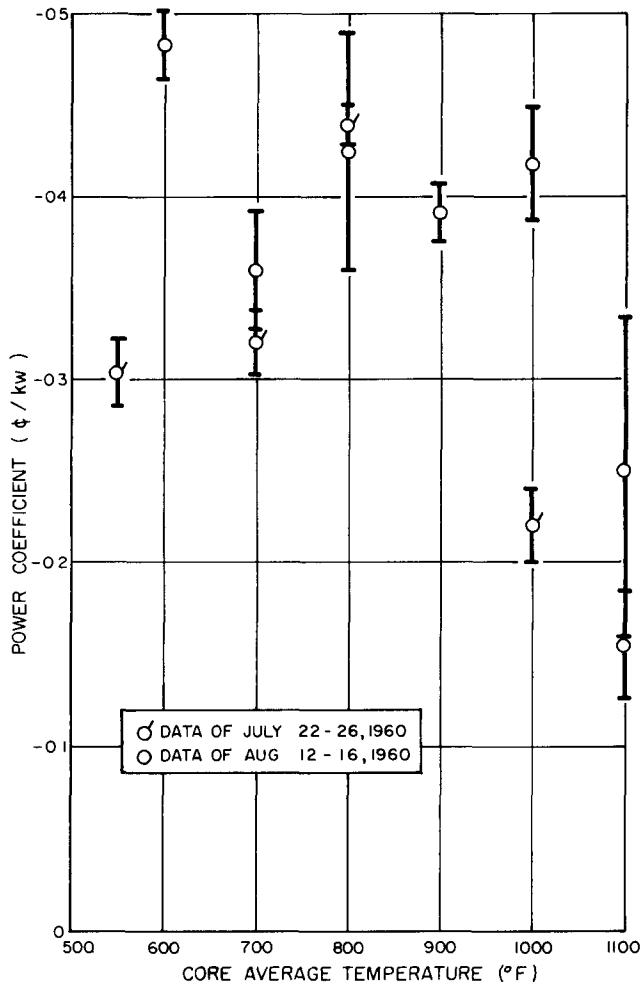

Figure 23. SER Power Coefficient vs Average Core Temperature

dependent upon temperature due to two effects. As the temperature increases, the size of the annular region between the fuel-moderator material increases, effecting an increase in dT_f/dp. Above temperature of 600°F, the evolution of hydrogen from the fuel-moderator in the annulus causing dT_f/dp to decrease. The net result of these two effects is to cause a decrease in the dT_f/dp term at temperatures above 600°F.

Thus, the decrease in the constant-inlet, constant-outlet power coefficient can be explained by a variation in the heat transfer coefficient of the fuel element with temperature. Since the absolute calculation of the heat transfer coefficient depends on a detailed knowledge of the as-built clad clearances and residual gas content of the annulus, it is impossible to assign a meaningful value to this parameter. The only conclusion that can be drawn from the power coefficient at constant core inlet and core outlet temperatures is that the results do not contradict values for the fuel element coefficient determined by other methods.

3. Ramp Reactivity Insertions

A set of studies was performed to attempt to separate the various components of the overall temperature coefficient of the SER. These studies consisted of placing the reactor on a positive period by the insertion of known amounts of reactivity by drum rotation at low power levels. The reactor power was allowed to increase until the reactivity insertion was compensated for by the increasing temperature. These studies were conducted with a variety of initial average core temperatures and flow conditions, including conditions of no flow. Typical curves resulting from these ramp insertions are shown in Figures 24 and 25.

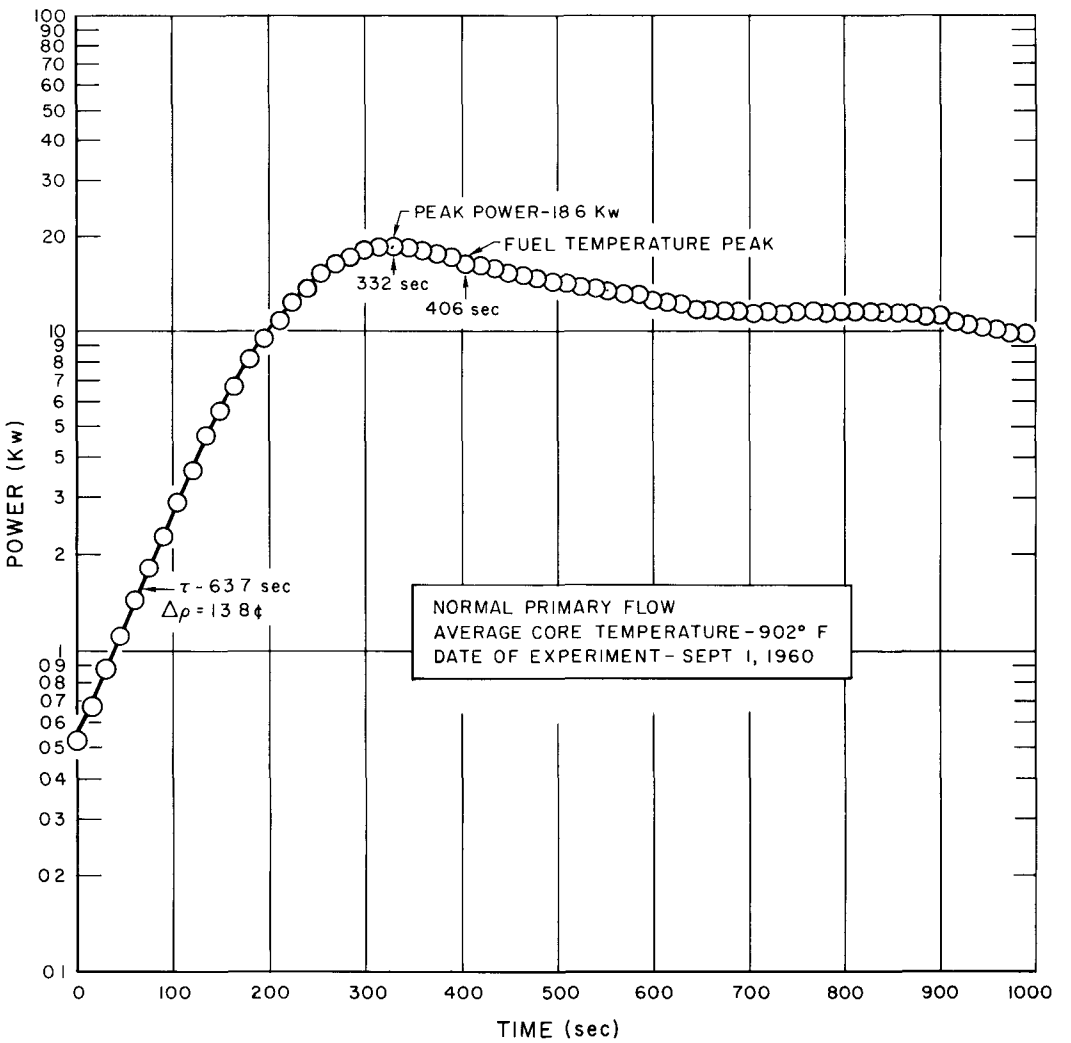

Figure 24. Ramp Insertion Experiment, kw vs Time

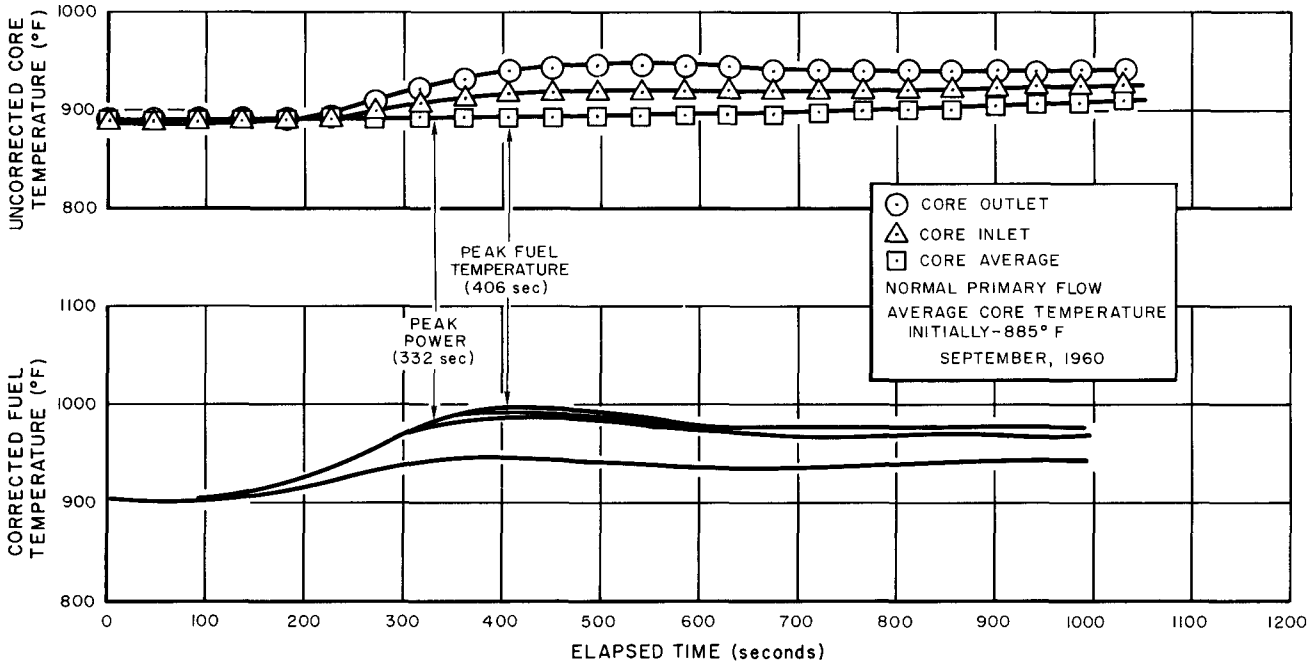

Figure 25. Ramp Insertion Experiment, Reactor Temperatures vs Time

Reactivity insertions were performed with no coolant flow, and with the coolant loop valve closed to limit convection of the coolant. It was hoped, in this manner, to limit the transfer of heat from the fuel to the other reactor components. The analysis of the transients was performed under the assumption that the only temperature coefficient acting during these transients was that associated with the fuel-moderator elements. These no-flow transients were analyzed by assuming that the reactor parameters could be represented by the following equations:

$$\frac{\ell}{B}\dot{P} = (\rho_o - \gamma\theta - 1)P + \sum \gamma_i H_i$$

$$\dot{H}_i = \lambda_i (P - H_i)$$

$$H_i = \frac{a_i B}{\lambda_i \ell} C_i$$

$$P = \delta \dot{\theta}$$

where

ℓ = prompt lifetime
B = delayed fraction
P = power in kw
ρ_o = initial reactivity input ($)
γ = temperature coefficient
θ = temperature rise during transient
a_i = fraction of delayed neutrons in i^{th} group
λ_i = decay constant for i^{th} group
C_i = delayed precursor population (kw units)
s = heat capacity of core

Assuming that, for the slow transients analyzed, the delayed precursor population peaks with the power; then, $\gamma\theta \cong \rho$ and

$$\gamma = \frac{-\rho^2 s(B/\ell)}{2P_{max}\left(1 + \frac{B}{\ell}\right)\sum \frac{a_i}{\lambda_i}}$$

where

$$\frac{B}{\ell} \cong 700,$$

and

$$\sum \frac{a_i}{\lambda_i} = 14.6,$$

Values of s range from 14 kw-sec/F° at 200°F to 20 kw-sec/F° at 1000°F; values of a_f were obtained for each no-flow transient performed. The results indicated a prompt temperature coefficient of ca. -0.04¢/F° over the temperature range 200 to 1000°F.

Another series of ramp insertions of reactivity were accomplished under varying flow conditions. The purpose of these experiments was to couple the effect of the grid plates into the reactivity compensation. These transients were studied by simulation of the reactivity input on an analog computer. The feedback terms of the analog were varied until the analogous power and temperature traces best matched those recorded from the reactor. A no-flow transient was also analyzed in this manner.

Results obtained from analog studies for no-flow conditions indicated a temperature coefficient of -0.065¢/F° which is attributable to the fuel-moderator elements. The coefficient implied from the studies made with flow indicates a value of -0.15¢/F° for both the grid plate and the fuel-moderator elements.

The values of the various coefficients contributing to the overall temperature coefficient are:

	Value (¢/F°)	Time Constant (sec)
Isothermal temperature coefficient	-0.35	-
Fuel-moderator temperature coefficient	~-0.05	10 - 20
Grid plate temperature coefficient (per plate)	~-0.10	1 - 5
Not accounted for by measurements (thought to be associated with external reflector)	-0.1	~1600

M. COMPARISON OF CALCULATED AND MEASURED SER PARAMETERS

(Calculated values taken from SER Hazards Report)

	Calculated	Measured
Excess reactivity	$7.77	$9.78
Fuel element worth in outer ring	$1.31	$1.40
Prompt temperature coefficient	-0.2¢/F°	~-0.05¢/F°
Overall temperature coefficient	-0.28¢/F°	-0.35¢/F°
Maximum fuel temperature (50 kw)	1250°F	1270°F
Control drum worth (one drum 0 - 180°)	$2.50	$3.65

VI. PROPOSED TESTS

In order to verify the stability and endurance capabilities of the SER, the reactor will be operated at design power and temperature to complete a total accumulated period of six months. In order to meet this requirement the SER will undergo an additional full-power operating period of six weeks. During this final period of operation additional tests will be undertaken. These tests will include the following:

A. STATIC POWER COEFFICIENTS

Further static power coefficient measurements at design temperature will yield another independent determination of the fuel temperature coefficient, a_f, and the upper grid plate coefficient, a_g. These measurements will be made somewhat differently than the previous ones. The following procedure will be used:

1) The reactor will be brought to design temperature, flow, and power;
2) A small change in reactivity will be made, and the resulting steady-state change in power will be recorded;
3) The inlet coolant temperature will be held constant; and
4) These conditions will be repeated at several different flow rates.

The steady-state reactivity inserted in such an experiment is given as:

$$\Delta\rho = a_{g_o}\Delta T_o + a_f\Delta\overline{T}_f + a_{iso}\Delta T_{in} \; ; \qquad \ldots(1)$$

where

$-a_{g_o}$ = upper grid plate coefficient,

$-a_f$ = fuel temperature coefficient,

$-a_{iso}$ = isothermal temperature coefficient,

ΔT_o = change in outlet temperature,

$\Delta\overline{T}_f$ = change in average fuel temperature,

ΔT_{in} = change in inlet temperature, and

$\Delta\rho$ = change in reactivity.

If the inlet is held constant ($\Delta T_{in} = 0$), the temperature changes are given as follows:

$$\Delta T_o = \frac{\Delta P}{W_c C_c} \qquad \text{and} \qquad \Delta \bar{T}_f = \frac{\Delta P}{UA} + \frac{\Delta P}{2 W_c C_c} \qquad \ldots (2)$$

where

W_c = coolant mass flow rate,

C_c = coolant heat capacity,

UA = heat transfer coefficient of fuel (average fuel to average coolant), and

ΔP = change in power.

Combining Equations 1 and 2 yields:

$$\frac{\Delta \rho}{\Delta P} = H_{P_{T_{in}, W_c}} = a_{g_o} \left(\frac{1}{W_c C_c} \right) + a_f \left(\frac{1}{2 W_c C_c} + \frac{1}{UA} \right)$$

where $H_{P_{T_{in}, W_c}}$ is defined as the prompt power coefficient at constant inlet temperature and constant flow. If several flow values are used, the measured prompt power coefficient $H_{P_{T_{in}, W_c}}$ can be plotted against $1/W_c C_c$ as shown in Figure 26. It is seen that the intercept of the curve is $\frac{a_f}{UA}$ and the slope is $a_{g_o} + \frac{a_f}{2}$. Thus, both the value of a_f and a_{g_o} may be determined providing the value of UA is known.

B. GRID PLATE COEFFICIENT

If the coolant flow rate is oscillated, a "cleaner" separation of the fuel and grid plate temperature coefficients can be obtained by taking advantage of their time response to a change in flow rate. Their response to a reactivity change is essentially the same because of the large fuel time constant, low coolant time constant, and low grid plate time constant. Their response to flow changes is considerably different, however. An instantaneous increase in flow causes a

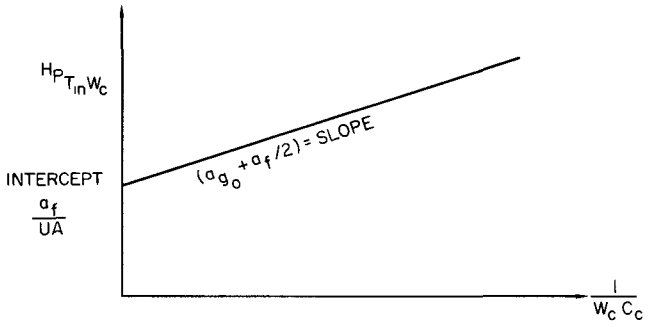

Figure 26. Reduction of Static Power Coefficient Measurements

very fast change in outlet temperature; however, the fuel responds more slowly because of its larger time constant. This difference in time behavior thus allows a more direct measure of the grid plate effects without having to make a large correction for the fuel temperature feedback effects.

To accomplish the instantaneous change in flow, a small sine wave oscillation is desirable; however, a sawtooth or trapezoidal wave is acceptable. A sawtooth wave can be obtained by varying the flow plus or minus 10% with a period of approximately 6 sec while recording the resulting perturbation of the inlet temperature, the outlet temperature, the fuel temperature, the power level, and the flux level. The data are reduced either on an analog computer or by using an analytical model. If an analog computer is used, the value of a_{g_o} is adjusted until the experimental power oscillation is matched. If the hand method is used, the fundamental Fourier components of the flow and power oscillation must be determined.

The test will be performed at near design temperature and power conditions.

C. REACTIVITY OSCILLATIONS

Although reactivity oscillation techniques have been used extensively to measure reactor parameters, the use of this method to determine the magnitude of the fuel and grid plate coefficients does not seem fruitful because the fuel and grid plate appear to respond almost simultaneously to a change in power level. The fuel has a large heat capacity and changes temperature slowly while the grid plate heats rapidly due to the rapid heat transport to it at high flow rates. At high oscillation frequencies, the fuel will not respond to power changes; hence, neither will the outlet coolant temperature. The static power coefficient measurements and the coolant oscillation tests discussed above appear to separate the two coefficients adequately.

The major value of a pile oscillation program is that it permits determination of the value of the fuel time constant; from which, the value of UA for the fuel can be determined. A secondary use of such a program may be to determine the effects of photoneutrons on the low power transfer function.

The theory of the method by which the measurement of the fuel time constant is determined can be illustrated by a simple analytical model of the reactor heat transfer process:

Fuel heat balance

$$M_f C_f \frac{d\overline{T}_f(t)}{dt} = P(t) - UA\left[\overline{T}_f(t) - \overline{T}_c(t)\right] ,$$

Coolant heat balance

$$M_c C_c \frac{d\overline{T}_c(t)}{dt} = UA\left[\overline{T}_f(t) - \overline{T}_o(t)\right] - W_c C_c \left[T_o(t) - T_{in}(t)\right]$$

$$\overline{T}_c(t) = \frac{T_o(t) + T_{in}(t)}{2} , \text{ and}$$

Reactivity expression

$$\rho(t) = -a_f \overline{T}_f(t) - a_{g_o} T_o(t) + \rho_o$$

where

M_f = fuel mass,

C_f = fuel heat capacity,

M_c = coolant mass,

C_c = coolant heat capacity,

$\overline{T}_f(t)$ = fuel average temperature,

$\overline{T}_c(t)$ = coolant average temperature,

$T_o(t)$ = outlet coolant temperature,

$T_{in}(t)$ = inlet coolant temperature, and

t = time.

The test procedure for this experiment would be as follows:

1) Oscillate a small amount of reactivity. A sinusoidal oscillation is most desirable from a data-reduction standpoint, but a trapezoidal or sawtooth oscillation may be used.

2) The oscillation must be done at the temperature level at which it is desired to make the measurement.

3) The experiment will be repeated at the same coolant temperature conditions but with reduced flow rates. Several frequencies of oscillation are also desirable.

The reduction of data can be done in several ways:

If an analog computer is used, the value of H_p must be inserted into the problem and the value of the effective time constant, T_R, may then be varied on the computer such as to reproduce the experimental power and reactivity traces. Data can also be reduced by hand by obtaining the fundamental Fourier components of the reactivity and flux oscillation. If a sawtooth or trapezoidal reactivity oscillation is used, the feedback transfer function can be obtained from this as follows:

$$\frac{T_{R}j\omega + 1}{H_p} = \frac{1}{G_{c1}(j\omega)} - \frac{1}{G_{R1}(j\omega)} \quad ;$$

where

ω = angular frequency = $2\pi f$,

$$G_{c1}(j\omega) = \frac{\text{Fundamental component of } (\Delta P)}{\text{Fundamental component of } (\Delta \rho)} \quad ,$$

and

$G_{R1}(j\omega)$ = zero power transfer function.

The value of $G_{R1}(j\omega)$ may be either calculated or measured. Several frequency points would allow a more precise determination of T_R and would tend to verify or disapprove the analytical model used.

If a trapezoidal reactivity oscillation is used for measuring the reactor time constant, the amplitude of the reactivity inserted or withdrawn should be approximately 5¢ and the period should be about 2 minutes.

D. REFLECTOR COEFFICIENT TEST

A large change in the coolant mean temperature may produce a measurable change in reactivity due to the beryllium reflector. This test will be conducted

at essentially zero power (100 watts). This test will be performed by producing a step decrease in the coolant mean temperature and by allowing the resulting change in reactivity to come to equilibrium. The reactivity following this change in coolant temperature should respond somewhat as shown in Figure 27.

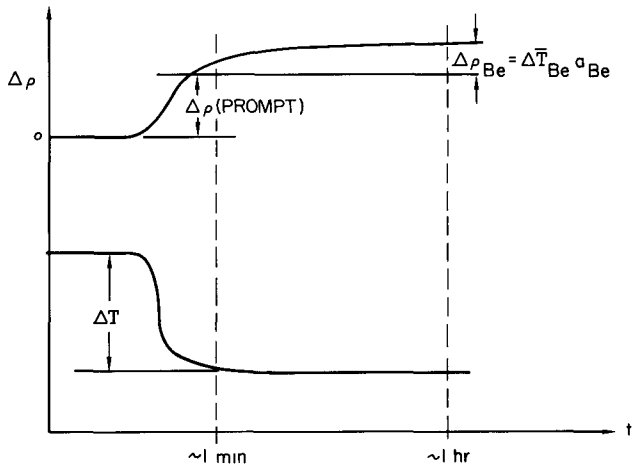

Figure 27. Estimated Response to Coolant Temperature Change

The initial rise in reactivity is due to the changes in grid plate and fuel temperatures. Any delayed effect can be deduced from the change in reactivity necessary to hold the reactor critical. Therefore, both the magnitude and time constant of any delayed effect can be determined.

A reasonably large change in mean coolant temperature (~200°F) is necessary to produce a reactivity change larger than that due to any system drifts. Performance of this test at essentially zero power will eliminate the need for xenon and other power coefficient corrections.

E. HYDROGEN LOSSES

During the final power run, the reactivity loss rate will be observed from day to day. By subtracting the known long-term reactivity losses, the loss attributed to hydrogen diffusion can be obtained. This figure will provide criteria for improving the effectiveness of vitreous enamel coatings for fuel-moderator assemblies of second generation SNAP-II assemblies.

F. CONTROL DRUM CALIBRATION

A final control drum calibration will be made at the completion of the six-week power run. This will not only furnish a check on the accuracy of the previous drum calibrations, but will also determine if there is any systematic change in drum worth that can be attributed to power operation.

This will complete the testing program for the SER. Sufficient data was obtained to permit the design of a second reactor of this general type, with improved characteristics.

VII. CONCLUSIONS

The design of the SER was undertaken to fill a real need for a small, compact power source for use in space vehicles. Present power sources severely limit the range and size of present space capsules. The successful operation of the SNAP-II Experimental Reactor under design conditions for the equivalent of a six-month operating period gives assurance that the development of small, compact nuclear reactors for use in space vehicles is not only feasible but practical.

The system has proven to be inherently stable and to have a negative power coefficient at all power levels, which minimizes the possibility of power excursions. It also facilitates reactor control under orbital conditions and ensures stable reactor operation over an extended period.

The only real maintenance problem encountered during the operation of the SER system was the NaK loop electrical heater which failed on two different occasions and caused an interruption in reactor operation while the heater bundle was being replaced. During the 1000-hr operation at design power and temperature, all process and nuclear instrumentation as well as the reactor and heat transfer systems functioned satisfactorily. This is further proof of the endurance capability of the SNAP-II system.

The primary function of the SER was to satisfactorily demonstrate the design concept and to determine the reactor parameters needed in the design of second-generation reactors. Sufficient data have been accumulated from the operation of the SER to enable the second phase of the SNAP-II program to proceed with confidence.

REFERENCES

1. R. R. Eggleston and G. L. Schmidt, "SNAP-II Experimental Reactor Hazards Report," NAA-SR-3465 (April 1, 1959)

2. G. H. Anno, "SNAP-II Environmental Test Facility Hazards Report," NAA-SR-3513 (May 1, 1959)

3. L. A. Wilson, "SNAP 2 Experimental Physics Analysis," NAA-SR-Memo-3607 (June 15, 1959)